LIF-dependent survival of embryonic stem cells is regulated by a novel palmitoylated Gab1 signalling protein

Linda Sutherland[1], Madeleine Ruhe[1], Daniela Gattegno-Ho[1], Karanjit Mann[1] Jennifer Greaves[2], Magdalena Koscielniak[1], Stephen Meek[1], Zen Lu[3*], Martin Waterfall[1], Ryan Taylor[1], Anestis Tsakiridis[4], Helen Brown[3], Sutherland K. Maciver[5], Anagha Joshi [1], Michael Clinton[1], Luke H. Chamberlain[2], Austin Smith[6] and Tom Burdon[1,#]

[1] Division of Developmental Biology, The Roslin Institute and R(D)VS, University of Edinburgh, Easter Bush, Midlothian, EH25 9RG, UK.

[2] Strathclyde Institute of Pharmacy and Biomedical Sciences, University of Strathclyde, Glasgow, G4 0RE, UK

[3] Division of Genetics and Genomics, The Roslin Institute and R(D)SVS

[4] Department of Biomedical Science, The University of Sheffield, E225, Alfred Denny Building, Western Bank, Sheffield, S10 2TN, UK

[5] Centre for Discovery Brain Sciences, Edinburgh Medical School, Biomedical Sciences, University of Edinburgh, Hugh Robson Building, George Square, Edinburgh, EH8 9XD, UK

[6] Wellcome Trust-Medical Research Council Stem Cell Institute, University of Cambridge, Tennis Court Road Cambridge, CB2 1QT, UK

[#] To whom correspondence should be addressed: Tom Burdon, Division of Developmental Biology, The Roslin Institute and R(D)VS, Easter Bush, Midlothian, EH25 9RG, UK Tel: +441316519169; tom.burdon@roslin.ed.ac.uk

***** Present address: PAPRSB Institute of Health Sciences, Universiti Brunei Darussalam, BE1410 Brunei Darussalam

JCS Advance Online Article. Posted on 28 August 2018

Keywords: Leukaemia inhibitory factor/Gab1/embryonic stem cells/palmitoylation/stem cell survival

Abstract

The cytokine leukaemia Inhibitory factor (LIF) promotes self-renewal of mouse embryonic stem cells (ESC) through activation of the transcription factor Stat3. However, the contribution of other ancillary pathways stimulated by LIF in ESCs, such as the MAPK and PI3K pathways, is less well understood. We show here that naïve-type mouse ESCs express high levels of a novel effector of the MAPK and PI3K pathways. This effector is an isoform of the Gab1 (Grb2-associated binder protein 1) adaptor protein that lacks the N-terminal Pleckstrin Homology (PH) membrane-binding domain. Although not essential for rapid unrestricted growth of ESCs under optimal conditions, the novel Gab1 variant (Gab1β) is required for LIF-mediated cell survival under conditions of limited nutrient availability. This enhanced survival is absolutely dependent upon a latent palmitoylation site that targets Gab1β directly to ESC membranes. These results show that constitutive association of Gab1 with membranes through a novel mechanism promotes LIF-dependent survival of murine ESCs in nutrient poor conditions.

Introduction

Embryonic stem cell (ESCs) are pluripotent cell lines derived from the inner cell mass of the blastocyst (Boeuf et al., 1997; Martello et al., 2013; Matsuda et al., 1999; Niwa et al., 1998; Niwa et al., 2009; Ye et al., 2013). They are immortal, differentiate into all foetal cell types *in vitro*, and most remarkably when reintroduced into an appropriately staged embryo reinitiate normal development to form all foetal tissues, including the germ line (Martello and Smith, 2014). These characteristics make ESCs a powerful experimental system and underpin their potential as a biomedical resource that can provide unlimited, scalable sources of normal cell-types for regenerative therapy and drug screening.

The biological capacity and value of ESCs relies upon the fidelity with which their developmental potential can be maintained in culture and as a consequence, considerable efforts have been made to understand the role of self-renewal signals and the transcriptional factors that maintain ESC pluripotency (Ying and Smith, 2017). The cytokine LIF plays a crucial role in promoting self-renewal of mouse ESCs and the signals it elicits have also been shown to have an important physiological role in supporting preimplantation mouse development (Nichols et al., 2001). Although the requirement for this cytokine in ESCs of other species is unclear, LIF is included as a supplement in culture media that support human stem cell lines thought to be equivalent to mouse ESCs, and non-rodent pluripotent stem cells can respond to LIF, suggesting that this cytokine signalling pathway may have a general role in supporting pluripotent stem cells of mammals (Guo et al., 2016; Takashima et al., 2014; Theunissen et al., 2014; Thomson et al., 2012).

LIF-dependent signalling is initiated by heterodimerization of LIF receptor with gp130, leading to cross-phosphorylation of receptor associated JAK tyrosine kinases. The activated kinases then phosphorylate specific receptor tyrosines that in turn serve as docking sites for the recruitment and activation of downstream effectors. The key effectors include the transcription factor Stat3, which activates expression of target genes directly, and the tyrosine protein phosphatase SHP2, which triggers the Erk MAPK cascade and

phosphatidylinositol 3-kinase (PI3K) signalling. Although studies have shown that Stat3 activation of the target genes Tfcp2L1, KLF4, and Gbx2 are critical for effective ESC self-renewal (Ying and Smith, 2017), the contribution of LIF activation of Erk MAPK and PI3K in ESC is less clear. Initial studies showed that the SHP2 activation was not essential for self-renewal and that general suppression of Erk MAPK signalling restricts mESC differentiation (Burdon et al., 1999). Indeed, suppression of Erk signalling when combined with activation of wnt/β-catenin signalling very effectively promotes self-renewal of undifferentiated ESCs (Buehr et al., 2008; Li et al., 2008; Wray et al., 2011; Ying et al., 2008). This 2-inhibitior (2i) culture system is enhanced further by the addition of LIF, suggesting that Stat3 or other LIF-induced signals are required to support efficient and robust propagation of ESCs (Dunn et al., 2014; Li et al., 2008; Ying et al., 2008).

A candidate mediator of LIF receptor signalling is Gab1 (Grb2-associated binder protein 1), an Insulin Receptor Substrate (IRS)/Daughter of Sevenless (DOS) family adaptor protein (Holgado-Madruga et al., 1996; Weidner et al., 1996). In common with other IRS/DOS proteins, Gab1 has no intrinsic enzymatic activity but functions as molecular scaffold to recruit and assemble signalling complexes. Gab1 is an important mediator of Erk, PI3K and PLC signalling induced by many growth factors - including the LIF/IL-6-related cytokines (Nishida and Hirano, 2003; Takahashi-Tezuka et al., 1998). The key functional elements of Gab1 include a membrane binding activity encoded by the N-terminal pleckstrin homology (PH) domain, and an extended unstructured C-terminal region that mediates protein-protein interactions with other signalling molecules. The 110 amino acid PH domain contains seven β-sheets capped off with a short amphipathic α-helix, forming a classic PH-fold that contains a binding site for the phospholipid product of PI3K, phosphatidylinositol (3,4,5)-triphosphate (PIP3) (Maroun et al., 1999a). Although initial recruitment of Gab1 to activated receptors is mediated through protein-protein interactions, tyrosine phosphorylation of Gab1 by receptor-activated kinases generates docking sites for PI3K, which in turn produces the PIP3 phospholipid ligand for the Gab1 PH domain. This PI3K/PH domain-dependent positive feedback loop stabilises the interaction between Gab1 and activated receptors and amplifies downstream

signals such as Erk via recruitment of SHP2 (Rodrigues et al., 2000). Previously we have shown that Gab1 is phosphorylated by activation of the gp130 receptor in mouse ESC (Burdon et al., 1999). Here we report the predominant form of Gab1 in mESCs is an unusual variant that lacks most of the conserved PH domain including the PIP3 phospholipid binding site. Nevertheless, we unexpectedly find that this novel form of Gab1 is constitutively associated with ESC membranes and specifically promotes LIF mediated ESC survival under conditions where nutrient availability is limited.

Results

A novel short form of the Gab1 adaptor protein is highly expressed in ESCs

Stimulation of mouse ESC via the gp130 cytokine receptor induces phosphorylation of the Gab1 adaptor protein (Burdon et al., 1999). However, the apparent molecular weight of Gab1 protein in mESCs, based on electrophoretic mobility, was significantly less than the 110-115 kDa reported for Gab1 protein of differentiated somatic cells (Burdon et al., 1999; Holgado-Madruga et al., 1996; Weidner et al., 1996). To understand the basis of this difference we compared Gab1 expression in mESC with other embryonic cell types by western blotting and found that the predominant form of Gab1 protein in ESC and embryonal carcinoma cells was ~95 kDa, whereas embryonic fibroblasts and pooled tissues of a mid-gestation embryo possessed the typical 110-115 kDa form (Fig. 1A). Coordinate downregulation of a 4.5 kb Gab1 RNA and the 95 kDa Gab1 protein during embryoid body differentiation implied that the short-form Gab1 was encoded by this ESC specific mRNA (Fig. S1A, B). We therefore sequenced Gab1 cDNAs obtained from an ESC cDNA library and found that all clones possessed a novel ~50 nucleotide non-coding 5' exon not present in the previously reported Gab1 cDNA, which is located ~ 20 kb downstream from the first exon containing the established Gab1 translation start codon (Fig. 1B S1C). Apart from the novel 5' non-coding exon, the predicted protein coding sequences of the ESC Gab1 cDNAs was identical to that previously reported for mouse Gab1, suggesting that translation of the ESC

Gab1 protein initiates at methionine codon downstream of the normal Gab1 start codon. To identify this novel start codon, we transiently transfected COS7 cells with a series of Gab1 cDNAs where translation was initiated at each of the first 4 in-frame ATG codons. Initiation at the most 5' methionine, M104, produced a Gab1 protein of similar mobility to that present in ESC protein lysates. (Fig. S1D). Methionine 104 is situated at the C-terminal boundary of the Gab1 PH domain (aa 10-117), and translation initiation from M104 eliminates most of this critical regulatory domain (Fig. 1C). The N-terminal located PIP3 binding site that mediates membrane localisation, and a less well characterised putative nuclear localisation sequence are also eliminated (Maroun et al., 1999b; Osawa et al., 2004). Nonetheless, the 95 kDa protein should retain all of the recognised direct protein-protein binding sites for partners such as Grb2, the MET receptor, PI3K and SHP2 and for our purposes will be referred to as Gab1β, to distinguish it from the previously characterised longer form, Gab1α.

To investigate how closely Gab1β expression was associated with the ESC state, we examined expression of the adaptor protein during induced pluripotent stem cell (iPSC) reprogramming of embryonic fibroblasts, and during exit from naive pluripotency to the "primed" pluripotent state representative of post-implantation epiblast stem cells (EpiSC). Western blotting showed that Gab1β was not expressed in partially reprogrammed pre-iPSCs (Fig. 1D), but was readily detected when cells transitioned to fully reprogrammed iPSCs derived either using standard serum/LIF, or the more stringent two inhibitor (2i) condition that promotes the 'naive' ESC ground state (Boroviak et al., 2014; Boroviak et al., 2015; Nichols and Smith, 2009). In contrast, Gab1β expression was absent from EpiSCs derived from post implantation embryos (Fig. 1D). The association of Gab1β with the naïve ESC state was further confirmed by monitoring the levels of Gab1 transcripts during the transition of an ESC line through a stable EpiSC state and into differentiated embryoid bodies (Fig.1E). Whereas expression of Gab1α increased as the ESCs transitioned to the primed state and then differentiated, Gab1β transcripts were sharply downregulated upon exit from the naïve ESC state, in line with the loss of Gab1β protein expression from the post-implantation epiblast derived cells (Fig

1D). Interestingly, these switches in Gab1 transcription are also reflected in changes in epigenetic status of putative Gab1 promoters (Fig S1E). In naïve ESCs, H3K4me3 histone methylation associated with active promoters is enriched at the region immediately upstream of the Gab1β first exon, whilst the Gab1α promoter region, by contrast, is enriched for the repressive H3K27me3 mark commonly associated with gene silencing.

To determine whether Gab1β was expressed during preimplantation development *in vivo* we performed RT-PCR amplification on mouse embryos and detected transcription of the novel 5' exon of Gab1β in both fertilised oocytes and blastocysts (Fig. S2A*)*. Gab1β transcription was also detected in primordial germ cells and western blotting indicated a low level expression of the 95 kDa protein in the adult testis (Fig. S2A, B*)*. By contrast, Gab1β protein was not readily detected in most other adult mouse tissues suggesting that high level expression was primarily restricted to ESCs and germ cells (Fig. S2B*)*.

Gab1 transcripts containing alternative 5' exons have also been found in EST cDNA libraries in animals ranging from frogs to humans (Fig. S1C). The corresponding Gab1β exon in mouse was identified by Cap-Analysis of Gene Expression (CAGE), a technique that maps 5' transcription initiation sites, providing evidence that a promoter within intron 1 drives expression of Gab1β (Fig. S2C). Transcription initiation at this site was also detected in trophoblast stem cell lines suggesting that while this variant form of Gab1 protein is enriched in ESCs, expression may not be exclusive to pluripotent cells of the early mouse embryo.

Gab1β promotes LIF-dependent signalling in ESCs

To evaluate the contribution of Gab1β to signalling in ESCs we first examined tyrosine phosphorylation of Gab1β in response to the growth factor supplements LIF and foetal calf serum used in routine ESC cultures (Fig. 2A, B). Western blotting of Gab1 immunoprecipitates showed that the overall level of Gab1β tyrosine phosphorylation increased only slightly in response to LIF or

serum. In contrast however, tyrosine phosphorylation at specific SHP2 (Y627) and PLCγ (Y307) binding sites increased markedly in response to LIF demonstrating that Gab1β is phosphorylated at recognised docking sites following stimulation of the LIF receptor. Consistent with this phosphorylation pattern, SHP2 immunoprecipitates from LIF-induced ESC contained Gab1β (Fig. 2B). Gab1β was also constitutively associated with the adaptor proteins p85 (non-catalytic subunit of PI3-Kinase), Grb2 and ShcA in ESCs (Fig. S3A, B).

Without the PH domain to stabilise association with the plasma membrane Gab1β might not be able to effectively propagate downstream signals since theoretically the adaptor protein should be unable to participate in the PH domain/PI3K/PIP3-dependent amplification mechanism (Rodrigues et al., 2000). Gab1β might even operate as a molecular sponge or decoy to dampen downstream effector functions. To determine how Gab1β influences downstream signalling we generated ESC lines that specifically lack Gab1β, but retain Gab1α expression. This was achieved by two consecutive rounds of homologous recombination with targeting vectors in which hygromycin and blasticidin resistance genes were inserted into the unique Gab1β 5' exon (Fig. S3C, D, E).

To assess the role of Gab1β in LIF signalling we examined phosphorylation of Akt, Erk and Stat3 in wild type ESCs, in Gab1β KO ESC, and in KO clones where we either restored Gab1β expression, or over-expressed Gab1α using stably integrated cDNA expression vectors (Fig. 2C). Whilst LIF-stimulated Stat3 phosphorylation was similar in all cell lines, the induction of Akt and Erk phosphorylation by LIF was noticeably reduced in Gab1β KO ESC compared with Gab1β wild-type ESC. However, reconstitution of Gab1β or over-expression of Gab1α in Gab1β KO cells increased both Akt and Erk phosphorylation compared with Gab1β KO cells. In contrast, Gab1β expression did not appear to play a significant role in serum-induced phosphorylation of Erk (Fig. S3F, G). These results demonstrated that despite not having a PH

domain, Gab1β contributes to signalling downstream of the LIF receptor in ESCs.

Gab1β expression provides a growth advantage in high density ESC cultures

To assess the biological function of Gab1β in ESC we first examined stem cell self-renewal, making use of the ESC-specific *Pou5f1*-βgeo knock-in allele in the IOUD2 parental ESC line, that allows the growth of undifferentiated stem cells to be monitored by measuring *Pou5f1*-LacZ derived β-galactosidase activity (Mountford et al., 1994). We compared β-galactosidase activity in wild-type and Gab1β KO IOUD2 cells in self-renewal assays and found that the cell lines exhibited similar levels of self-renewal in response to different concentrations of LIF (Fig. S4A), indicating that Gab1β expression did not affect ESC self-renewal at the low cell densities used in these self-renewal assays.

To investigate whether Gab1β expression affects ESC growth at higher cell densities we examined the behaviour of Gab1β-deficient ESCs in near confluent cultures. We used Gab1β mutant cell lines generated from the standard wild-type E14Tg2a parental cells (Fig S4B, C), to exclude concerns that genetic modification of the *Pou5f1* gene might affect the response of cells in high density assays (Karwacki-Neisius et al., 2013). Consistent with the previous IOUD2 experiments, self-renewal assays in the E14Tg2a Gab1β expressing and deficient KO lines did not reveal consistent differences between lines (Fig. S4D). When we plated two independent Gab1β heterozygous and two Gab1β KO E14Tg2a clones at densities typical of those routinely used for propagating ESC lines (~10^5 cells/cm^2) the initial growth of the cell lines was indistinguishable in the first 2-3 days. However, once the lines approached confluence it appeared that the survival of Gab1β expressing heterozygous cells was noticeably greater than that of the Gab1β KO cells (Fig 3A). Monitoring ESC growth by measuring live cell DNA-dependent fluorescence daily throughout a 6-day culture period confirmed that the growth of all four clones was very similar for the first 2 days. However, between the 3rd and 4th

days, when cell growth slowed, the Gab1β expressing heterozygous cells attained higher cell numbers and maintained these higher levels for an extended period (Fig. 3B). Statistical analysis showed that from day 3 onwards, the mean live cell DNA fluorescence differed significantly between the Gab1β heterozygous and KO cells. To confirm that this effect was due to Gab1β expression we repeated the growth experiments using pools of Gab1β KO cells stably transfected with either a Gab1β expression vector or an EGFP control, and compared them with a pool of Gab1β heterozygous clones transfected with a mCherry expression control vector (Fig. 3C). As with previous experiments, the cell lines showed similar rates of growth during the first two days, but between days 3-4 the Gab1β restored and heterozygous cells exhibited a growth or survival advantage over the KO cells lacking Gab1β. There was a statistically significant difference between the live cell DNA fluorescence in EGFP control and Gab1β expressing cells between day 4-6, but not between the Gab1β heterozygous mCherry-transfected cells and Gab1β expressing cells. Collectively, these results establish that Gab1β expression provides a growth or survival advantage in high cell density culture conditions.

Gab1β promotes ESC survival in nutrient depleted conditions

To determine the cause of the growth advantage associated with Gab1β expression we examined cell proliferation and apoptosis in the near-confluent ESC cultures. The cell cycle profiles of Gab1β expressing and non-expressing cells were determined by measuring DNA content by flow cytometry. The overall profiles were indistinguishable during either the rapid or plateau growth phases, although as expected, there was a noticeable reduction in the S-phase contribution in both cell types during the plateau phase (Fig. 4A). However, it was evident that Gab1β KO cells accumulated a greater amount of sub-diploid/fragmented cells at day 3 during the plateau growth phase, pointing to increased levels of cell death in these cultures (Fig. 4A, B). We therefore used flow cytometry to assess the level of apoptosis by measuring the percentage of live cells that were positive for the apoptotic maker Annexin V. While equivalent

levels of early apoptosis were observed at day 1 in both ESC cultures, at day 2 there was a marked increase in Annexin V staining in the Gab1β-deficient KO cells, (Fig. 4C). Caspase 3/7 activation and cytotoxicity, reflecting general cell death, were both noticeably higher in the day 2/3 Gab1β KO cultures further supporting the notion that absence of Gab1β was associated with increased levels of apoptosis (Fig. 4D). Taken together these results suggest that expression of the Gab1β protein in ESCs promotes cell survival when culture conditions become restrictive.

In high-density cultures a number of factors including environmental, physical or metabolic might limit ESC growth. To distinguish between these alternatives we modified the culture environment and monitored the effects on ESC growth. To investigate what factors affect the growth profile, we treated ESC with an inhibitor of the enzyme mTOR (mammalian/mechanistic target of rapamycin), a key enzyme that senses and controls nutrient availability in cells, and is a regulator of anabolic process such as protein, lipid and nucleotide synthesis (reviewed in (Saxton and Sabatini, 2017)) . Addition of 25 nM mTOR inhibitor (INK128) restricted the initial growth rate of Gab1β expressing and non-expressing cells equally and reduced the maximum cell numbers achieved in both cases (Fig 5A). Under these restrictive conditions the growth/survival advantage of the Gab1β expressing cells was still apparent, even though it occurred at a lower cell numbers, implying that it was unlikely that cell density was responsible for limiting the later phase of ESC growth.

To determine whether nutrients might be limiting the growth of Gab1β–deficient ESCs, we tested how supplementation with medium components affected ESC culture growth and survival at the plateau phase (Fig 5B, C). Addition of either standard DMEM, or DMEM lacking glucose, sodium pyruvate and glutamate at day 2 of the culture improved the survival of Gab1β KO ESCs, suggesting that depletion of amino acids or vitamin supplements common to both growth media become limiting for ESC growth during the plateau phase, and excluded the depletion of energy sources such as glucose as being directly responsible for slowing ESC growth. Direct supplementation of plateau phase cultures with

glutamine or sodium pyruvate also did not appreciably improve ESC survival/growth, (Fig. S5).

Gab1β mediated ESC survival is LIF-dependent

We have shown that Gab1β is phosphorylated after stimulation of the LIFR, and activates downstream signalling (Fig. 2). To determine whether LIF signalling was also required for Gab1β-mediated ESC survival in nutrient-depleted cultures we compared the growth of Gab1β expressing and non-expressing cells with or without LIF during the 6-day cultures. Whereas cells in all conditions grew rapidly for the first two days, in both Gab1β expressing and KO cultures deprived of LIF cell numbers declined rapidly after this point in a manner similar to that displayed by Gab1β KO cells cultured in the presence of LIF (Fig. 6A). This demonstrated that ESC survival in post-confluent cultures relies on LIF signalling, and is also effected by Gab1β expression. Although unlikely, it is possible that the loss of cell viability seen here is a result of ESC differentiation initiated by LIF withdrawal. To address this possibility, we restricted ESC differentiation by including the Mek inhibitor PD0325901 in the LIF-deficient high density cultures. However, this did not improve ESC survival (Fig. 6A), and may even have compounded the effects of LIF withdrawal. To explore the relationship between Gab1β and LIFR-mediated cell survival, we examined the LIF dose response of ESC cultures (Fig. S6 A, B). Whereas the survival of the Gab1β expressing cells at the plateau phase was dependent on the dose of LIF, the acute collapse in viability of the majority of the Gab1β KO cells was largely dose-independent.

Survival of Gab1β KO ESCs is rescued by inhibition of FGFR or Mek activity

The studies above were performed under standard serum + LIF culture conditions, but we were interested in determining how Gab1β expression might affect ESC growth and survival under culture conditions, such as 2i+LIF, that

selectively promote the naïve ESC state. We found that while cell proliferation in the initial growth phase was similar to that in serum-containing medium (Fig. 6B), in the post-plateau phase, Gab1β KO cell survival in 2i+LIF medium was markedly better than in serum +LIF medium, and comparable to cells expressing Gab1β. There were differences in growth characteristics of ESCs in 2i+LIF serum-free and serum + LIF media - with 2i+LIF cells forming more compact and tight colonies. Nonetheless these results indicate that conditions induced by 2i+LIF compensate for the absence of Gab1β in the Gab1β KO cells. To determine how 2i+LIF contributes to this "rescue" effect we inhibited either Mek or its upstream activator FGFR (fibroblast growth factor receptor) in the standard serum +LIF conditions. Treatment of cells with Mek inhibitor or the FGFR inhibitor PD173074 had little effect on the initial rate of expansion of ESCs but in both cases improved the survival of the Gab1β KO cells (Fig. 6C, D). Taken together these results indicate that the survival function of Gab1β and the inhibition of FGFR/Mek dependent activities converge to promote ESC survival.

Gab1β is located at ESC membranes

Localisation of Gab1 at the cell membrane is thought to be critical for its functional activity and yet, despite lacking an intact PH domain, Gab1β contributes to ESC signalling and promotes ESC survival. To understand how Gab1β could influence ESC survival without the PH domain, we examined the cellular location of Gab1β in ESCs. Based on previous reports a Gab1 protein lacking the phospholipid binding site contained within the PH domain should be located in the cytoplasm (Maroun et al., 1999b; Rodrigues et al., 2000). However, when we compared the location of Gab1 protein in wild-type and Gab1β KO ESC by immunocytochemistry (using the antibody that recognises both Gab1α and β forms), it was clear that in wild-type cells a significant proportion of Gab1 protein was at the cell membrane (Fig. 7A). By contrast, in Gab1β KO cells there was very little membrane-associated Gab1 protein (Fig. 7B). Crucially, stable expression of a Gab1β cDNA in the KO cells restored the

wild-type distribution of Gab1, demonstrating that Gab1β in ESCs is normally located at the cell membrane (Fig. 7C).

To determine how Gab1β is directed to the membrane we examined the cellular localisation of Gab1-EGFP fusion proteins stably expressed in the Gab1β KO cells. Whereas the Gab1β-EGFP fusion protein carrying EGFP at the C-terminus of Gab1β was located predominantly at the ESC membrane (Fig. 7D), the corresponding Gab1α-EGFP protein was largely cytoplasmic, with only a minority of ESCs displaying membrane associated Gab1α-EGFP (Fig. 7E). Significantly, a fusion protein in which EGFP was attached to the N-terminus of Gab1β was entirely cytoplasmic (Fig. 7F). This result suggested that the membrane targeting signal of Gab1β can be blocked by attachment of EGFP, or the PH domain, and is therefore is likely to be located close to the N-terminus of the protein.

Gab1 proteins that lack the entire PH domain (amino acids 10-117) have been shown to be located in the cytoplasm (Maroun et al., 1999b; Rodrigues et al., 2000). However, these artificial mutants are not directly comparable to Gab1β expressing cells as we noted that the N-terminus of Gab1β retains an additional 15 amino acids (15 aa) from the end of the PH domain. This 15 amino acid polypeptide forms a structurally conserved amphipathic helix that typically caps off PH domains (Lemmon and Ferguson, 2000). To examine the contribution of this 15 aa polypeptide we deleted this element from the Gab1β-EGFP fusion protein and found in agreement with previous reports (Maroun et al., 1999b; Rodrigues et al., 2000) the Gab1β-Δ15aa-EGFP protein was located in the cytoplasm (Fig. 7G). To examine directly how the N-terminal region of Gab1β contributes to membrane targeting, we examined the localisation of EGFP fusion proteins carrying the N-terminal 47 amino-acids (aa104-150) or just the 15 amino acid peptide (104-118) of Gab1β (Fig. 7H, I). The 47aa-EGFP protein was very clearly located at the membrane. In comparison, the 15aa-EGFP fusion protein exhibited a weaker signal at the membrane and evidence of irregular distribution throughout the cytoplasm. Taken together these experiments suggest that the N-terminal region of Gab1β, containing the residual 15 aa alpha helical region derived from the PH domain, is sufficient to

target Gab1β to the ESC membrane. Gab1β protein also accumulated at an intracellular site in most ESCs (Fig. 7 A, C), as did the Gab1β-EGFP and 47aa-EGFP fusion proteins (Fig. 7D,H) indicating that Gab1β may also associate with the membranes of intracellular vesicles.

Palmitoylation of Gab1β drives its membrane localisation and function

Our localisation experiments demonstrate that the 15 aa N-terminus of Gab1β contains a signal that targets it to ESC membranes. Examination of this region identified three cysteines that were potential sites for palmityolyation, a lipid modification that could account for the stable association of Gab1β with the cell membrane (Fig. 8A). The three cysteines are conserved to different extents amongst Gab family members, including the Gab1 homolog DOS present in *Drosophila,* and SOC-1 in *Caenorhabditis*. To test directly whether Gab1β is palmitoylated in ESCs, we cultured ESCs expressing Gab1-EGFP fusion proteins in the presence of ^{3}H-palmitate and examined ^{3}H-labelling of EGFP immunoprecipitates after electrophoresis and transfer to an immobilising filter. Autoradiography revealed that Gab1β and the 47aa fusion constructs were labelled efficiently with ^{3}H-palmitate (Fig. 8B). By contrast, deletion of the 15aa region from Gab1β, or alanine substitution of the three cysteines in 47aa fusion protein (47aa-CA3m-EGFP), prevented labelling. Interestingly, ^{3}H-labeling of Gab1α or Gab1 PH domain-EGFP fusion proteins could not be detected, demonstrating that in the presence of the intact PH domain Gab1 palmitoylation is suppressed or at least was inefficient under these experimental conditions. To determine how palmitoylation of Gab1 affects membrane targeting, we examined the localisation of the 47aa-CA3 mutant–EGFP in ESC and found that alanine substitution of the three cysteines in this mutant abolished membrane targeting of the fusion protein (Fig. 8C). Significantly, the identical alanine substitutions within the context of the PH domain-EGFP fusion protein did not prevent localisation at the membrane (Fig. 8C).

These results strongly suggest that palmitoylation of the N-terminal domain drives membrane localisation of Gab1β in ESC. We therefore determined whether palmitoylation of Gab1β was also associated with supporting ESC survival. We compared the growth of Gab1β KO ESCs with cells stably expressing cDNAs encoding either Gab1β or a Gab1β-CA3 mutant. In contrast to cells expressing wild-type Gab1β, ESCs expressing the Gab1β-CA3 mutant protein exhibited the same growth profile as the Gab1β KO cells, showing that the palmitoylation of Gab1β and localisation at the ESC membrane is required for Gab1β-dependent ESC survival in culture (Fig. 8D).

Discussion

LIF receptor/gp130 signalling has essential roles during early embryonic development that provide the physiological rationale for the contribution of this signalling pathway to the growth and self-renewal of embryonic stem cells (ESCs) in culture (Do et al., 2013; Nichols et al., 2001). Here we report the identification of a novel variant form of the adaptor protein Gab1 (Gab1β) that contributes to LIF-dependent survival of ESCs under conditions of limited nutrient availability. In this Gab1 variant the domain that normally regulates the access of the protein to the membrane and to activated receptors is replaced by a lipid tag that anchors the Gab1β adaptor protein constitutively at the cell membrane. Although disruption of *Gab1* expression does not normally disturb pre-gastrulation embryo development, we presume the switch in regulatory modes may confer an additional growth or survival advantage under exceptional circumstances (Itoh et al., 2000; Sachs et al., 2000). Since Gab1β is expressed in cells representative of the early preimplantation epiblast and the trophoblast stem cell compartment, we speculate that a primary function of Gab1β is to support preimplantation embryos exposed to suboptimal environmental conditions in the uterus.

The abundance of Gab1β protein and its phosphorylation following treatment with LIF pointed to the adaptor protein having a functional role in ESCs. Under the standard clonal culture conditions typically used to assess growth and self-renewal, ESCs tolerated the loss of Gab1β. However, when challenged with nutrient-limited conditions, Gab1β expression reduced cell death and extended the viability of ESCs. When cells were treated with an inhibitor of the key nutrient sensor and anabolic regulatory enzyme mTOR Gab1β expression improved ESC survival, which could imply that availability of nutrients is a contributory limiting factor. Indeed, rescue of starved ESC cultures by supplementation with minimal basal medium indicated that either lack of amino acids or vitamins was responsible for collapse of the cultures. It has been reported that restricting ESC growth induces a state that resembles the quiescent condition induced in embryos during delayed implantation (also known as diapause) (Renfree and Shaw, 2000). In the natural condition, preimplantation blastocysts undergo developmental arrest and implantation is delayed in order to synchronise embryo development with the mother's reproductive capacity and environmental inputs. Importantly, inhibition of mTOR is reported to suppress ESC growth and to maintain a "paused" quiescent, but developmentally competent, state in ESCs and blastocysts for over a week (Bulut-Karslioglu et al., 2016). This suggests that nutrient availability may determine entry into this quiescent condition and this state can be induced experimentally in culture.

The survival function of Gab1β in ESCs was evident in LIF treated cultures. Gab1β expression also increased LIFR-mediated Erk and Akt phosphorylation, implicating the adaptor directly as a transducer of LIF receptor signals. PI3K/Akt signalling has been shown to be involved in Gab1-mediated cell survival and in ESCs activation of this pathway has been reported to promote cell growth, survival and self-renewal (Cherif et al., 2015; Fan et al., 2016; Fukumoto et al., 2009; Furuta et al., 2016; Hishida et al., 2015; Holgado-Madruga and Wong, 2003; Holgado-Madruga et al., 1997; Jirmanova et al., 2002; Paling et al., 2004; Sun et al., 2014; Watanabe et al., 2006). By contrast, Erk activation is normally associated with ESC differentiation, and inhibition of Mek/Erk signalling promotes ESC self-renewal (Burdon et al., 1999; Ying et al., 2008). Notably,

inhibition of either FGFR or Mek activity improved the survival of Gab1β-KO ESCs, and appeared to largely rescue the Gab1β deficiency. Indeed, it has been reported that Mek inhibition reduces the requirement for PI3K signalling in ESC, thus potentially uncoupling cells from the requirement for PI3K-dependent survival signals provided by Gab1β (Hishida et al., 2015). A possible alternative explanation is that Gab1β might represent a physiological disruptor of Mek signalling by altering the activation kinetics of the pathway, or by binding Erk and regulating access of this kinase to its target proteins (Osawa et al., 2004; Wolf et al., 2015).

Membrane localisation of Gab1β is essential for its survival function and is dependent on palmitoylation of this ESC adaptor protein. The lipid modification targets Gab1β to ESC membranes, liberating Gab1β from dependence on PI3K activity and availability of the phospholipid PIP3, and locates the adaptor in close proximity to upstream effectors such as receptors and associated kinases. Removal of the PH domain also eliminates an auto-inhibitory interaction between the PH domain and C-terminal region of Gab1 (Eulenfeld and Schaper, 2009; Wolf et al., 2015). This blocks PIP3 binding by the PH domain, but can be relieved by Erk-mediated phosphorylation of the C-terminal domain. Freed from this regulatory constraint, Gab1β should be constitutively available to associate with receptors and maintain the basal level of Gab1β phosphorylation observed in ESCs. Nonetheless, Gab1β cannot participate in the PH domain/PI3K/PIP3 positive feedback loop and therefore will be limited in its capacity to amplify downstream signalling. Understanding why Gab1β expression is preferred in ESCs rather than simply upregulating Gab1α expression should provide insights into how quantitative and qualitative aspects of signalling affect cell behaviour in the early embryo. Perhaps direct association of Gab1β with the cell membrane increases sensitivity to LIF receptor/gp130 mediated activation, but limits the intensity and duration of signalling to curb differentiation or proliferation - thus supporting stem cell survival under growth restrictive conditions.

Gab variants with alternative N-terminal sequences have been described previously. A hamster Gab1 protein (Gab1$^{\Delta 1\text{-}103}$) analogous to Gab1β, enhances anchorage-independent growth of preneoplastic fibroblasts (Kameda et al., 2001), and PH-domain deficient isoforms have also been reported for the closely related Gab-family member Gab2 (Adams et al., 2012; Gu et al., 1998; Gu et al., 2001). Interestingly, membrane localisation of another IRS/DOS family member, Fibroblast Growth Factor Receptor Substrate 2 (FRS2) depends upon myristylation to target this adaptor protein to the cell membrane and enable its participation in downstream signalling (Kouhara et al., 1997). Gab protein variants may therefore exemplify a more general mechanism for diversifying the intracellular locations of this class of adaptor proteins and their contribution to signalling.

Gab1β is highly expressed in " ground state" naive ESCs that are thought to closely represent the epiblast of the preimplantation embryo (E3.75-E4.5) (Boroviak et al., 2014). Interestingly, although Gab1β expression is down-regulated during the transition to form EpiSCs, a cell type representing the post-implantation epiblast (Brons et al., 2007; Tesar et al., 2007), high levels of Gab1β transcription are also detected in trophoblast stem cells. This may indicate that Gab1β transcription is regulated by factors common to both epiblast and trophoblast stem cells, and additionally point to Gab1β having a broader role in regulating the viability of cells within the whole preimplantation embryo.

In conclusion, Gab1β is highly expressed in rodent ESCs and supports LIF-dependent survival when nutrient availability becomes limiting. How Gab1β and its downstream effectors interact with the regulatory machinery of cells in the preimplantation embryo, and their relevance to conditions prevalent *in vivo* deserves further consideration and could provide new insights into the control of embryo survival.

Materials and Methods

Cell culture and transfections

ESCs were cultured without feeder cells in Glasgow modification of Eagle's medium (GMEM) containing 10% foetal calf serum, 0.1 mM 2-mercaptoethanol and LIF as described previously (Chambers et al., 2003; Hooper et al., 1987; Mountford et al., 1994; Niwa et al., 2000; Smith, 1991). R2 pre-iPS cells were cultured on irradiated DIAM feeders (Meek et al., 2010) in GMEM/FCS (Theunissen et al., 2011). iPS cells were cultured in 2i+LIF medium (Theunissen et al., 2011) or with GMEM/FCS/LIF as described for ESC above. EpiSC cells were grown on fibronectin coated plates in N2B27 medium containing Activin (20 ng/ml) and FGF2 (12 ng/ml) (Guo et al., 2009; Osorno et al., 2012). PSMB embryonal carcinoma, primary mouse embryonic fibroblasts, COS7, NIH 3T3 and C3H 10T1/2 cells were maintained in ESC culture medium without LIF. For routine ESC culture LIF was generated in house. For inductions and growth experiments ESGRO recombinant Mouse LIF protein (ESG1107) was obtained from Merck. The small molecule inhibitors PD0325901 (#1408) and CHIR99021 (#1386) were obtained from Axon Medchem, and PD173074 (S1264) from Selleckchem.

COS7 were transfected using the Fugene 6 transfection reagent in accordance with the manufacturer's instructions (Roche Molecular Biochemicals) at approximately 50% confluence, were incubated for 72 hrs with 2 μg of supercoiled plasmid DNA complexed with 5 μl Fugene and then harvested for protein analysis. Transfected ESC were obtained by incubating the cells (0.5-1 x 10^6 cells per well of 6-well dish) with 5 μg of plasmid DNA using Lipofectamine 2000 reagent (Life Technologies) for 36 hours. ESC clones stably transfected with Gab1 expression vectors were selected in ESC medium containing Puromycin (1 μg/ml) or Hygromycin (100 μg/ml) (for 10 days, then trypsinised and combined to establish pooled cultures for each construct. For growth factor induction experiments ESCs were cultured overnight in GMEM base medium lacking glutamine and serum prior to stimulation with growth factors. E14/T cells

were super-transfected with supercoiled plasmids carrying the polyoma origin of replication as described previously.

Cloning Gab1 cDNAs and expression constructs

The mouse Gab1α cDNA was generated by RT-PCR using a Superscript preamplification system (Invitrogen) to reverse transcribe 1ug of total RNA from C3CH10T1/2 fibroblasts. 1/10th of the reaction was amplified using Expand High fidelity polymerase (Roche) with 5' GGGCGGCCGCCGCACC**ATGAGCGGTGGTGAAGTG** and 3' CCCTCGAG**TCACTTCACATTCTTGGTGGGTG** oligonucleotide primers containing Not1 and Xho1 restriction sites respectively (underlined). Thirty cycles of PCR generated the expected 2 kb DNA fragment, which was restricted with Not1 and Xho1, subcloned and sequenced. Gab1β cDNAs were isolated from an ESC cell cDNA library provided by Dr Hitoshi Niwa. Three independent clones were sequenced at their 5' and 3' ends and one clone sequenced on both strands of the coding region. Gab1α and Gab1β cDNAs were restricted with Not1 and Xho1 and subcloned into pCAGIH a hygromycin resistant derivative of the pCAGIZ expression vector (Jackson et al., 2002; Niwa et al., 1998). This plasmid contains the SV40 origin sequence, allowing efficient transgene expression in cells harbouring the SV40 large T antigen. A progressively truncated series of Gab1 cDNAs, M104, M151, M232, and M240 were generated by PCR amplification. Reactions were performed with a 5' primer containing a Not1 restriction site and Kozak consensus immediately upstream of the ATG initiation codon plus 16-19 nucleotides of downstream Gab1 sequence and a 3' primer containing an Xho1 restriction site. The amplified products were subcloned into the pCAGIH expression vector as Not1/Xho1 fragments. Gab1-EGFP or Gab1-myc tagged fusion proteins were generated by PCR amplification of Gab1 regions cloned in pCAGIH (or puro version pCAGIP) modified vectors, upstream of a an open reading frame containing either a poly glycine- EGFP protein, or a triple myc-tag respectively. The 15aa N-terminal region of Gab1β was cloned upstream of EGFP as a double stranded oligonucleotide. The sequences of the oligonucleotide primers used to generate the Gab1 coding regions are available on request. Gab1

expression vectors were linearised with Sfi1 prior to transfections. Drug resistant ESC colonies were picked individually or pooled to establish stably transfected cultures.

Preparation of embryonic RNA and RT-PCR analysis

Embryos and cells were prepared from appropriately staged 129 female mice. After flushing from the oviduct, oocytes were treated with hyaluronidase to remove cumulus cells. Both oocytes and blastocysts were washed extensively to eliminate contaminating cellular debris prior to lysis. Primordial germ cells (PGCs) were isolated from the dissected genital ridges of day 12.5 embryos, using calcium and magnesium free phosphate buffered saline (Buehr and McLaren 1993). Freshly prepared oocytes (n=35), blastocysts (n=30) and PGCs were lysed in Solution D and RNA was purified by acid phenol extraction (Chomczynski and Sacchi, 1987). To aid recovery of RNA, 20 μg of carrier tRNA was added to the samples prior to extraction. cDNA was prepared from 1/5th of the recovered RNA using random priming and the Superscript Preamplification system. 1/10th of the reverse transcription reaction was then amplified using AmpliTaq Gold polymerase (Perkin Elmer). PCR reactions of 50 cycles were performed using primers that amplify a 184 bp DNA fragment from Gab1β cDNA (GGACCATTCGAGGTGGCAGAC; CAACCCAGCATCAACTTGCTGAC) or a 939 bp DNA fragment from β-actin cDNA (GTGACGAGGCCCAGAGCAAGAG; AGGGGCCGGACTCATCGTACTC).

Disruption of Gab1β expression by homologous recombination

Genomic DNA spanning the Gab1β exon was obtained by screening the RPC121 Mouse PAC library obtained from UK HGMP Resource Centre (Osoegawa et al., 2000) with the ^{32}P end-labelled Gab1β oligonucleotide TACTCAGGTGTCATGCGTCTGCCACCTCGAATGGT. A ~ 7 kb Xba1 DNA fragment encompassing the Gab1β exon was isolated from the PAC clone 340-d21, cloned into pBS and sequenced using the Genome Priming System (New England Biolabs). ET-cloning using bacterial recombination was used to introduce a kanamycin gene into the Gab1β exon to create a unique BamH1

site into which a PGK polyadenylation signal was cloned (Muyrers et al., 1999). This sequence was amplified with a 5' primer incorporating BamH1 and Sal1 restriction sites and 3' primer containing a Bgl11 site. Hygromycin, and blasticidin selection markers were then individually cloned as BamH1, Sal1 fragments immediately upstream of the PGK sequence to generate three targeting vectors. Plasmid was digested with Xba1, to free the targeting vector from the plasmid backbone, prior to transfections. In transfections either 1 x 10^8 ESC were electroporated (800V, 3 μF) with 150 μg linearised plasmid or 1 x 10^7 cells were electroporated (240 V, 500 μF) with 40 μg linearised plasmid. Cells were plated at 2-3 x 10^6 cells per 10 cm dish and 48 hours later treated with medium containing either Blasticidin (10 μg/ml), Hygromicin (100 μg/ml) or G418 (200 μg/ml). After ~ 10 days selection colonies were picked and expanded for freezing and DNA analysis. Genomic DNA was prepared from clones grown to confluency in 24-well plates using Proteinase K digestion followed by isopropanol precipitation. Approximately 1/5th of the resuspended DNA was restricted with EcoRV , transferred to an uncharged Nylon filter (Amersham) by Southern blotting and hybridised with DNA probes, located either 5' or 3' of the targeting construct, generated by PCR (5' probe primers: AGAGTCCTGTTGTATGCCTGG, CAAGTACTCCTTACTGCCCAG; 3' probe primers: GACTCACCAGAAATGGGGTTC, AGGTGATGTGGTTTCATGTAG) .

ESC Self-renewal assays

To compare stem cell self-renewal between wild-type and Gab1 mutant IOUD2 cells Oct4-β-galactosidase activity was quantitated as described previously (Burdon et al., 1999). ESC were plated in 24 well plates (5000 cells/well), cultured for 6-days and β-galactosidase activity in lysates was measured using the ONPG assay. Specific enzyme activity was normalised relative to the protein concentration of lysates and standardised against a serial dilution of purified β-galactosidase enzyme (Promega). Triplicate samples were assayed as duplicates.

Alkaline phosphatase activity was assayed in ESC lysates prepared from cells in 24-well plates (described above), using 1 ml of 1 mM $MgCl_2$/0.2% NP-40 per well and incubated for 2 hours at 37ºC. Duplicate aliquots (80 μl) were mixed

with 10 μl Glycine buffer (1M Glycine, 10 mM $ZnCl_2$, 10 mM $MgCl_2$), and 10 ml of 100 mM p-nitrophenyl phosphate (Sigma), incubated in a 96-well plate for 20-60 minutes and the absorbance was read at 405 nM.

Cell growth/proliferation assay

Cells were plated onto uncoated tissue culture 96-well plates at 20,000 or 40,000 cells per well in 100 μl of growth medium, and cell growth was assayed using the CyQuant Direct Cell Proliferation Assay (C35011 ThermoFisher Scientific) to measure live cell associated DNA fluorescence. Each sample, was assayed by addition of 100 μl of 2x detection reagent (0.4 μl Direct DNA stain, 2 μl Direct Background suppressor diluted in 100 μl Opti-MEM ThermoFisher Scientific 11058021), incubated for 1 hr at 37^0C in the incubator and then read on Victor Multi Label Counter from the bottom of plates with standard green filter at 508/527 nM excitation/emission wavelengths. Each cell line sample or treatment was measured in a minimum of four independent wells for each experiment.

Cell cycle analysis

Single cell suspensions of cells were fixed in 70% ethanol, rehydrated in phosphate buffered saline for 30 mins at 4^o, rinsed twice with PBS and then incubated with 100 μg DNAse free RNAse for 1 hr at room temperature. Propidium iodide (final concentration 50 μg/ml) was added to the cells for 10 minutes before flow analysis (Fortessa X-20, Becton Dickinson: 561 nM laser, emission 610 nM). Data was acquired using FACSDiva software (Becton Dickinson). The cytometer was set to linear fluorescence for optimal resolution for DNA, and data collected for 50,000 events per sample. The percentages of G0, G1, S and G2 phases were manually determined using FlowJo 10 software.

Apoptosis and cytotoxicity assays

Single cell suspensions containing 1 x 10^5 cells/sample, as well as apoptosis control treated with Staurosporine (1 μM: 1 hr), and dead cell control (2% DMSO: 1 hr) were stained using the Annexin V – APC Kit (Biolegend) according to the manufacturer's instructions. Cells were washed once with Annexin V

Binding buffer, then resuspended in 100 μl of the same buffer and stained using 5 μl Annexin V reagent. Samples were incubated for 15 minutes in the dark and then diluted with 400 μl binding buffer and adjusted to 50 mg/ml Propidium Iodide, prior to flow analysis on a Fortessa cytometer (Becton Dickinson: 640 nM laser, emission 670 nM). Data analysis was carried out using FlowJo 10 software.

For assessing Apoptosis/Cytotoxicity/Viability we used the ApoTox-Glow Triplex Assay (Promega G6320) according to the manufacturer's instructions. Cells were plated at 40,000 cells in 100 μl medium, per well of tissue culture 96-well plates and grown for 2 further days. The Viability/Cytotoxicity reagent (20 μl) was added to each well, mixed by orbital shaking and incubated for 30 minutes at 37^0C and then read at 405 nM (excitation)/505 nM (emission) for Viability, and 485 nM (excitation)/ 520 nM (emission) using a BioTek Synergy Ht plate reader. To measure apoptosis, Caspase-Glo reagent (100 ml) was added to each well, mixed by orbital shaking, incubated at room temperature for 30 minutes and the luminescence was read using the Biotek Synergy Ht plate reader. Ethanol (0.7%: 1 hr) and Staurosporine (1 mM: 1 hr) treated cells served as cell death and apoptosis controls respectively.

Northern analysis of RNA

RNA was prepared from cells lysed in acid guanidinium hydrochloride (Chomczynski and Sacchi, 1987). Northern blots were produced from samples containing 10 μg of total RNA probed with the ^{32}P-labeled Gab1α cDNA.

Quantitative reverse transcriptase PCR

RNA (1 μg) purified using RNeasy Mini Kit (Qiagen) was used to sythesise cDNA using SuperScript First-Strand Synthesis System (Invitrogen). Approximately 1/60th of the cDNA was amplified using Platinum SYBR Green QPCR kit (Invitrogen) using the conditions; 50^{o}C for 2 minutes then 95^{o}C for 2 minutes followed by 40 cycles of 95^{o}C for 15s then 60^{o}C for 30s, with a final cycle consisting of 95^{o}C for 1 minute, 60^{o}C for 30s and 95^{o}C for 15s. Gab1 isoform specific forward primers were: α GGAGAAGAAGTTGAAGCGTTA, β GACGCATGACACCTGAGTA. The common reverse primer was:

GCAACACAAACCACCTTCT. β-actin control primers were: forward TGACAGGATGCAGAAGGAGA, reverse GTACTTGCGCTCAGGAGGAG.

Immunoprecipitation and Immunoblotting

Immunoprecipitations were performed essentially as described previously (Burdon et al., 1999). ESC (5 x 10^6) were plated overnight in 10 cm diameter dishes. The cells were serum and cytokine starved for 24 hrs prior to induction with growth factors. Cells were lysed in 0.6mls ice-cold lysis buffer (150 mM NaCl, 10 mM Tris-HCl, pH 7.4, 0.5% NP40, 1 mM $NaVO_4$, 1 mM EDTA, 0.5 mM PMSF), cleared of nuclear and cytoplasmic debris and then incubated with ~1μg antibody and protein A sepharose for 4-16 hrs at 4^0C. Immune complexes were washed extensively and then boiled in SDS-sample buffer prior to gel electrophoresis. For protein analysis in whole cell lysates, ESC were plated at 5 x 10^6 cells per well in 6-well dishes. After plating overnight and a further 24 hours in serum-free medium, cells were stimulated with growth factors, washed once with PBS and lysed in 100 or 200 μl of SDS-sample buffer. These lysates were sonicated and boiled prior to loading on gels. Following electrophoresis on 8 or 10% denaturing SDS-polyacrylamide gels, proteins were electroblotted onto ECL-nitrocellulose filters (Amersham) and probed with antibodies (diluted 1:1000). The antibodies used in this study were obtained from New England Biolabs/Cell Signalling Technology: phospho-Erk # 9101; phospho-Akt (Ser473) #4058, phospho Gab1 Tyr307 #3234; phospho Gab1 Tyr627 # 3231; phospho Stat3 #9131, #9138 BD/Transduction Labs: Erk2 E16220; Stat3 S21320; Grb2 G16720, Upstate Biotechnology: phosphotyrosine 4G10, Gab1 CT #06-579; p85 #06-195, Santa Cruz: SHP2 sc-280; Myc sc-40; Oct4 sc-5279 . A rabbit polyclonal anti-Gab1 antibody was very generously provided by T. Hirano and M. Hibi (Takahashi-Tezuka et al., 1998).

Immunocytochemistry and Confocal microscopy

Approx 1 x 10^6 cells in 500 μl of medium were allowed to attach to glass coverslips (pretreated with 1% gelatin) in the bottom of a 6-well culture dish for 1 hour. Wells were then flooded with medium and the cells cultured overnight. Cell on the cover slips were fixed for 10 minutes in 4% paraformaldehyde at

room temperature, gently washed 5 times with PBST (PBS, 0.03% TritonX-100), and then incubated with blocking solution (PBST, 3% goat serum, 1% BSA) for one hour at room temperature. Primary antibodies were diluted in blocking solution and applied overnight at 4ºC, followed by four washes with PBST. Appropriate secondary antibodies were diluted 1:1000 in blocking solution and applied for one hour, at room temperature in the dark. The cells were washed extensively with PBST, and the final wash contained 10µg/ml DAPI. The antibodies used were Oct4 primary antibody at 1:200 (Santa Cruz, sc5279) with goat-anti-mouse IgG2b secondary antibody, rabbit anti-Gab1 antibody (gift of T. Hirano) at 1:500 (Takahashi-Tezuka et al., 1998). The coverslips were then laid over the depression in a concave microscope slide filled with 150 µl PBS and imaged using a Nikon EC1 confocal microscope at 60x magnification. For imaging live cells on microscope slides, cells were maintained in Opti-MEM (Life Technologies).

3H palmitate labelling

Transfected cells were incubated for 4 hours in media containing 0.5mCi/ml 3H palmitic acid (Perkin Elmer) and 0.1% BSA (fatty acid-free). The GFP-tagged proteins were then immunoprecipitated with magnetic microbeads coupled to GFP antibody (Miltenyi Biotech). Immunoprecipitated proteins were separated by SDS-PAGE and transferred to nitrocellulose membranes. ^{3}H-palmitate present on the recovered GFP-tagged proteins was detected using a Kodak Biomax Transcreen LE intensifier screen.

Statistical Methods

Cell growth data was analysed using mixed models to allow for random variability in the group effects occurring between the replicate experiments. The models fitted: group, day and the group.day interaction as fixed effects; and replicate, replicate.group, replicate.day and replicate.group.day as random effects. A different residual variance was allowed for each day of the trial, after checking this led to a significant improvement in the model compared to a model

using a constant residual variation, using a likelihood ratio test. In order to satisfy normality assumptions, a log transformation of the data was used for all analyses except that for Figure 3b where a square root transformation was preferable. t-tests were defined with the models to carry out pairwise comparisons of specified groups on each day of the trial.

Acknowledgements

We are indebted to following scientists for their help, advice and provision of samples: Jitsutaro Kawaguchi, Christopher Greenhalgh, Jose Silva, Jennifer Nichols, Keisuki Kaji, Joseph Mee, Kay Samuel, Valerie Wilson, Toshio Hirano, Masahiko Hibi, Robert Flemming, David Waddington, and the staff at ISCR and Roslin. AS is a Medical Research Council Professor. This work was funded with support from the Biotechnology and Biological Sciences Research Council.

Author Contribution.

LS, MR, DG-H, KM, JG, MS, SM, ZL, MW, RT, AT, AJ and TB performed experiments. TB, MC, LC, HB and AS analysed the data. TB, AS, SM, LC provided guidance and/or senior supervision. TB and MC wrote the manuscript. TB prepared the figures. All authors appraised the manuscript and figures.

Conflict of Interest

No competing interests declared

References

Adams, S. J., Aydin, I. T. and Celebi, J. T. (2012). GAB2--a scaffolding protein in cancer. *Mol. Cancer Res.* **10**, 1265–1270.

Boeuf, H., Hauss, H., De Graeve, F., Baran, N. and Kedinger, C. (1997). Leukemia inhibitory factor-dependent transcriptional activation in embryonic stem cells. *J. Cell Biol.* **138**, 1207–1217.

Boroviak, T., Loos, R., Bertone, P., Smith, A. and Nichols, J. (2014). The ability of inner-cell-mass cells to self-renew as embryonic stem cells is acquired following epiblast specification. *Nat. Cell Biol.* **16**, 516–528.

Boroviak, T., Loos, R., Lombard, P., Okahara, J., Behr, R., Sasaki, E., Nichols, J., Smith, A. and Bertone, P. (2015). Lineage-Specific Profiling Delineates the Emergence and Progression of Naive Pluripotency in Mammalian Embryogenesis. *Dev. Cell* **35**, 366–382.

Brons, I. G., Smithers, L. E., Trotter, M. W., Rugg-Gunn, P., Sun, B., Chuva de Sousa Lopes, S. M., Howlett, S. K., Clarkson, A., Ahrlund-Richter, L., Pedersen, R. A., et al. (2007). Derivation of pluripotent epiblast stem cells from mammalian embryos. *Nature* **448**, 191–195.

Buehr, M., Meek, S., Blair, K., Yang, J., Ure, J., Silva, J., McLay, R., Hall, J., Ying, Q.-L. and Smith, A. (2008). Capture of authentic embryonic stem cells from rat blastocysts. *Cell* **135**, 1287–98.

Bulut-Karslioglu, A., Biechele, S., Jin, H., Macrae, T. A., Hejna, M., Gertsenstein, M., Song, J. S. and Ramalho-Santos, M. (2016). Inhibition of mTOR induces a paused pluripotent state. *Nature* **540**, 119–123.

Burdon, T., Stracey, C., Chambers, I., Nichols, J. and Smith, A. (1999). Suppression of SHP-2 and ERK signalling promotes self-renewal of mouse embryonic stem cells. *Dev. Biol.* **210**, 30–43.

Chambers, I., Colby, D., Robertson, M., Nichols, J., Lee, S., Tweedie, S.

and Smith, A. (2003). Functional expression cloning of nanog, a pluripotency sustaining factor in embryonic stem cells. *Cell* **113**, 643–655.

Cherif, M., Caputo, M., Nakaoka, Y., Angelini, G. D. and Ghorbel, M. T. (2015). Gab1 Is Modulated by Chronic Hypoxia in Children with Cyanotic Congenital Heart Defect and Its Overexpression Reduces Apoptosis in Rat Neonatal Cardiomyocytes. *Biomed Res. Int.* **2015**, 718492.

Chomczynski, P. and Sacchi, N. (1987). Single-step method of RNA isolation by acid guanidinium thiocyanate-phenol-chloroform extraction. *Anal. Biochem.* **162**, 156–159.

Do, D. V., Ueda, J., Messerschmidt, D. M., Lorthongpanich, C., Zhou, Y., Feng, B., Guo, G., Lin, P. J., Hossain, M. Z., Zhang, W., et al. (2013). A genetic and developmental pathway from STAT3 to the OCT4-NANOG circuit is essential for maintenance of ICM lineages in vivo. *Genes Dev.* **27**, 1378–90.

Dunn, S.-J., Martello, G., Yordanov, B., Emmott, S. and Smith, A. G. (2014). Defining an essential transcription factor program for naïve pluripotency. *Science* **344**, 1156–60.

Eulenfeld, R. and Schaper, F. (2009). A new mechanism for the regulation of Gab1 recruitment to the plasma membrane. *J. Cell Sci.* **122**, 55–64.

Fan, Y., Yang, F., Cao, X., Chen, C., Zhang, X., Zhang, X., Lin, W., Wang, X. and Liang, C. (2016). Gab1 regulates SDF-1-induced progression via inhibition of apoptosis pathway induced by PI3K/AKT/Bcl-2/BAX pathway in human chondrosarcoma. *Tumour Biol.* **37**, 1141–9.

Fukumoto, T., Kubota, Y., Kitanaka, A., Yamaoka, G., Ohara-Waki, F., Imataki, O., Ohnishi, H., Ishida, T. and Tanaka, T. (2009). Gab1 transduces PI3K-mediated erythropoietin signals to the Erk pathway and regulates erythropoietin-dependent proliferation and survival of erythroid cells. *Cell. Signal.* **21**, 1775–83.

Furuta, K., Yoshida, Y., Ogura, S., Kurahashi, T., Kizu, T., Maeda, S., Egawa, M., Chatani, N., Nishida, K., Nakaoka, Y., et al. (2016). Gab1

adaptor protein acts as a gatekeeper to balance hepatocyte death and proliferation during acetaminophen-induced liver injury in mice. *Hepatology* **63**, 1340–55.

Gu, H., Pratt, J. C., Burakoff, S. J. and Neel, B. G. (1998). Cloning of p97/Gab2, the major SHP2-binding protein in hematopoietic cells, reveals a novel pathway for cytokine-induced gene activation. *Mol. Cell* **2**, 729–740.

Gu, H., Saito, K., Klaman, L. D., Shen, J., Fleming, T., Wang, Y., Pratt, J. C., Lin, G., Lim, B., Kinet, J. P., et al. (2001). Essential role for Gab2 in the allergic response. *Nature* **412**, 186–190.

Guo, G., Yang, J., Nichols, J., Hall, J. S., Eyres, I., Mansfield, W. and Smith, A. (2009). Klf4 reverts developmentally programmed restriction of ground state pluripotency. *Development* **136**, 1063–1069.

Guo, G., von Meyenn, F., Santos, F., Chen, Y., Reik, W., Bertone, P., Smith, A. and Nichols, J. (2016). Naive Pluripotent Stem Cells Derived Directly from Isolated Cells of the Human Inner Cell Mass. *Stem cell reports* **6**, 437–46.

Hishida, T., Nakachi, Y., Mizuno, Y., Katano, M., Okazaki, Y., Ema, M., Takahashi, S., Hirasaki, M., Suzuki, A., Ueda, A., et al. (2015). Functional compensation between Myc and PI3K signaling supports self-renewal of embryonic stem cells. *Stem Cells* **33**, 713–25.

Holgado-Madruga, M. and Wong, A. J. (2003). Gab1 is an integrator of cell death versus cell survival signals in oxidative stress. *Mol. Cell. Biol.* **23**, 4471–4484.

Holgado-Madruga, M., Emlet, D. R., Moscatello, D. K., Godwin, A. K. and Wong, A. J. (1996). A Grb2-associated docking protein in EGF- and insulin-receptor signalling. *Nature* **379**, 560–564.

Holgado-Madruga, M., Moscatello, D. K., Emlet, D. R., Dieterich, R. and Wong, A. J. (1997). Grb2-associated binder-1 mediates phosphatidylinositol 3-kinase activation and the promotion of cell survival

by nerve growth factor. *Proc. Natl. Acad. Sci. U. S. A.* **94**, 12419–24.

Hooper, M., Hardy, K., Handyside, A., Hunter, S. and Monk, M. (1987). HPRT-deficient (Lesch-Nyhan) mouse embryos derived from germline colonization by cultured cells. *Nature* **326**, 292–295.

Itoh, M., Yoshida, Y., Nishida, K., Narimatsu, M., Hibi, M. and Hirano, T. (2000). Role of Gab1 in heart, placenta, and skin development and growth factor- and cytokine-induced extracellular signal-regulated kinase mitogen- activated protein kinase activation. *Mol. Cell. Biol.* **20**, 3695–3704.

Jackson, M., Baird, J. W., Cambray, N., Ansell, J. D., Forrester, L. M. and Graham, G. J. (2002). Cloning and characterization of Ehox, a novel homeobox gene essential for embryonic stem cell differentiation. *J. Biol. Chem.* **277**, 38683–38692.

Jirmanova, L., Afanassieff, M., Gobert-Gosse, S., Markossian, S. and Savatier, P. (2002). Differential contributions of ERK and PI3-kinase to the regulation of cyclin D1 expression and to the control of the G1/S transition in mouse embryonic stem cells. *Oncogene* **21**, 5515–5528.

Kameda, H., Risinger, J. I., Han, B. B., Baek, S. J., Barrett, J. C., Abe, T., Takeuchi, T., Glasgow, W. C. and Eling, T. E. (2001). Expression of Gab1 lacking the pleckstrin homology domain is associated with neoplastic progression. *Mol. Cell. Biol.* **21**, 6895–6905.

Karwacki-Neisius, V., Göke, J., Osorno, R., Halbritter, F., Ng, J. H., Weiße, A. Y., Wong, F. C. K., Gagliardi, A., Mullin, N. P., Festuccia, N., et al. (2013). Reduced Oct4 expression directs a robust pluripotent state with distinct signaling activity and increased enhancer occupancy by Oct4 and Nanog. *Cell Stem Cell* **12**, 531–45.

Kouhara, H., Hadari, Y. R., Spivak-Kroizman, T., Schilling, J., Bar-Sagi, D., Lax, I. and Schlessinger, J. (1997). A lipid-anchored Grb2-binding protein that links FGF-receptor activation to the Ras/MAPK signaling pathway. *Cell* **89**, 693–702.

Lemmon, M. A. and Ferguson, K. M. (2000). Signal-dependent membrane targeting by pleckstrin homology (PH) domains. *Biochem. J.* **350**, 1–18.

Li, P., Tong, C., Mehrian-Shai, R., Jia, L., Wu, N., Yan, Y., Maxson, R. E., Schulze, E. N., Song, H., Hsieh, C.-L., et al. (2008). Germline competent embryonic stem cells derived from rat blastocysts. *Cell* **135**, 1299–310.

Maroun, C. R., Holgado-Madruga, M., Royal, I., Naujokas, M. A., Fournier, T. M., Wong, A. J. and Park, M. (1999a). The gab1 PH domain is required for localization of gab1 at sites of cell-cell contact and epithelial morphogenesis downstream from the met receptor tyrosine kinase. *Mol. Cell. Biol.* **19**, 1784–1799.

Maroun, C. R., Moscatello, D. K., Naujokas, M. A., Holgado-Madruga, M., Wong, A. J. and Park, M. (1999b). A conserved inositol phospholipid binding site within the pleckstrin homology domain of the Gab1 docking protein is required for epithelial morphogenesis. *J. Biol. Chem.* **274**, 31719–31726.

Martello, G. and Smith, A. (2014). The nature of embryonic stem cells. *Annu. Rev. Cell Dev. Biol.* **30**, 647–75.

Martello, G., Bertone, P. and Smith, A. (2013). Identification of the missing pluripotency mediator downstream of leukaemia inhibitory factor. *EMBO J.* **32**, 2561–74.

Matsuda, T., Nakamura, T., Nakao, K., Arai, T., Katsuki, M., Heike, T. and Yokota, T. (1999). STAT3 activation is sufficient to maintain an undifferentiated state of mouse embryonic stem cells. *EMBO J.* **18**, 4261–4269.

Meek, S., Buehr, M., Sutherland, L., Thomson, A., Mullins, J. J., Smith, A. J. and Burdon, T. (2010). Efficient gene targeting by homologous recombination in rat embryonic stem cells. *PLoS One* **5**, e14225.

Mountford, P., Zevnik, B., Duwel, A., Nichols, J., Li, M., Dani, C., Robertson, M., Chambers, I. and Smith, A. (1994). Dicistronic targeting

constructs: reporters and modifiers of mammalian gene expression. *Proc. Natl Acad. Sci. USA* **91**, 4303–4307.

Muyrers, J. P., Zhang, Y., Testa, G. and Stewart, A. F. (1999). Rapid modification of bacterial artificial chromosomes by ET-recombination. *Nucleic Acids Res.* **27**, 1555–1557.

Nichols, J. and Smith, A. (2009). Naive and primed pluripotent states. *Cell Stem Cell* **4**, 487–492.

Nichols, J., Chambers, I., Taga, T. and Smith, A. (2001). Physiological rationale for responsiveness of mouse embryonic stem cells to gp130 cytokines. *Development* **128**, 2333–9.

Nishida, K. and Hirano, T. (2003). The role of Gab family scaffolding adapter proteins in the signal transduction of cytokine and growth factor receptors. *Cancer Sci.* **94**, 1029–1033.

Niwa, H., Burdon, T., Chambers, I. and Smith, A. (1998). Self-renewal of pluripotent embryonic stem cells is mediated via activation of STAT3. *Genes Dev.* **12**, 2048–2060.

Niwa, H., Miyazaki, J. and Smith, A. G. (2000). Quantitative expression of Oct-3/4 defines differentiation, dedifferentiation or self-renewal of ES cells. *Nat. Genet.* **24**, 372–6.

Niwa, H., Ogawa, K., Shimosato, D. and Adachi, K. (2009). A parallel circuit of LIF signalling pathways maintains pluripotency of mouse ES cells. *Nature* **460**, 118–122.

Osawa, M., Itoh, S., Ohta, S., Huang, Q., Berk, B. C., Marmarosh, N. L., Che, W., Ding, B., Yan, C. and Abe, J. (2004). ERK1/2 associates with the c-Met-binding domain of growth factor receptor-bound protein 2 (Grb2)-associated binder-1 (Gab1): role in ERK1/2 and early growth response factor-1 (Egr-1) nuclear accumulation. *J. Biol. Chem.* **279**, 29691–29699.

Osoegawa, K., Tateno, M., Woon, P. Y., Frengen, E., Mammoser, A. G.,

Catanese, J. J., Hayashizaki, Y. and de Jong, P. J. (2000). Bacterial artificial chromosome libraries for mouse sequencing and functional analysis. *Genome Res.* **10**, 116–128.

Osorno, R., Tsakiridis, A., Wong, F., Cambray, N., Economou, C., Wilkie, R., Blin, G., Scotting, P. J., Chambers, I. and Wilson, V. (2012). The developmental dismantling of pluripotency is reversed by ectopic Oct4 expression. *Development* **139**, 2288–2298.

Paling, N. R., Wheadon, H., Bone, H. K. and Welham, M. J. (2004). Regulation of embryonic stem cell self-renewal by phosphoinositide 3-kinase-dependent signaling. *J. Biol. Chem.* **279**, 48063–48070.

Renfree, M. B. and Shaw, G. (2000). Diapause. *Annu. Rev. Physiol.* **62**, 353–375.

Rodrigues, G. A., Falasca, M., Zhang, Z., Ong, S. H. and Schlessinger, J. (2000). A novel positive feedback loop mediated by the docking protein Gab1 and phosphatidylinositol 3-kinase in epidermal growth factor receptor signaling. *Mol. Cell. Biol.* **20**, 1448–1459.

Sachs, M., Brohmann, H., Zechner, D., Muller, T., Hulsken, J., Walther, I., Schaeper, U., Birchmeier, C. and Birchmeier, W. (2000). Essential role of Gab1 for signaling by the c-Met receptor in vivo. *J. Cell Biol.* **150**, 1375–1384.

Saxton, R. A. and Sabatini, D. M. (2017). mTOR Signaling in Growth, Metabolism, and Disease. *Cell* **168**, 960–976.

Smith, A. G. (1991). Culture and differentiation of embryonic stem cells. *J. Tiss. Cult. Meth.* **13**, 89–94.

Sun, L., Chen, C., Jiang, B., Li, Y., Deng, Q., Sun, M., An, X., Yang, X., Yang, Y., Zhang, R., et al. (2014). Grb2-associated binder 1 is essential for cardioprotection against ischemia/reperfusion injury. *Basic Res. Cardiol.* **109**, 420.

Takahashi-Tezuka, M., Yoshida, Y., Fukada, T., Ohtani, T., Yamanaka, Y.,

Nishida, K., Nakajima, K., Hibi, M. and Hirano, T. (1998). Gab1 acts as an adapter molecule linking the cytokine receptor gp130 to ERK mitogen-activated protein kinase. *Mol. Cell. Biol.* **18**, 4109–4117.

Takashima, Y., Guo, G., Loos, R., Nichols, J., Ficz, G., Krueger, F., Oxley, D., Santos, F., Clarke, J., Mansfield, W., et al. (2014). Resetting transcription factor control circuitry toward ground-state pluripotency in human. *Cell* **158**, 1254–69.

Tesar, P. J., Chenoweth, J. G., Brook, F. A., Davies, T. J., Evans, E. P., Mack, D. L., Gardner, R. L. and McKay, R. D. (2007). New cell lines from mouse epiblast share defining features with human embryonic stem cells. *Nature* **448**, 196–199.

Theunissen, T. W., van Oosten, A. L., Castelo-Branco, G., Hall, J., Smith, A. and Silva, J. C. (2011). Nanog overcomes reprogramming barriers and induces pluripotency in minimal conditions. *Curr. Biol.* **21**, 65–71.

Theunissen, T. W., Powell, B. E., Wang, H., Mitalipova, M., Faddah, D. A., Reddy, J., Fan, Z. P., Maetzel, D., Ganz, K., Shi, L., et al. (2014). Systematic identification of culture conditions for induction and maintenance of naive human pluripotency. *Cell Stem Cell* **15**, 471–487.

Thomson, A. J., Pierart, H., Meek, S., Bogerman, A., Sutherland, L., Murray, H., Mountjoy, E., Downing, A., Talbot, R., Sartori, C., et al. (2012). Reprogramming pig fetal fibroblasts reveals a functional LIF signaling pathway. *Cell Reprogr.* **14**, 112–122.

Watanabe, S., Umehara, H., Murayama, K., Okabe, M., Kimura, T. and Nakano, T. (2006). Activation of Akt signaling is sufficient to maintain pluripotency in mouse and primate embryonic stem cells. *Oncogene*.

Weidner, K. M., Di Cesare, S., Sachs, M., Brinkmann, V., Behrens, J. and Birchmeier, W. (1996). Interaction between Gab1 and the c-Met receptor tyrosine kinase is responsible for epithelial morphogenesis. *Nature* **384**, 173–176.

Wolf, A., Eulenfeld, R., Bongartz, H., Hessenkemper, W., Simister, P. C.,

Lievens, S., Tavernier, J., Feller, S. M. and Schaper, F. (2015). MAPK-induced Gab1 translocation to the plasma membrane depends on a regulated intramolecular switch. *Cell. Signal.* **27**, 340–52.

Wray, J., Kalkan, T., Gomez-Lopez, S., Eckardt, D., Cook, A., Kemler, R. and Smith, A. (2011). Inhibition of glycogen synthase kinase-3 alleviates Tcf3 repression of the pluripotency network and increases embryonic stem cell resistance to differentiation. *Nat. Cell Biol.* **13**, 838–845.

Ye, S., Li, P., Tong, C. and Ying, Q.-L. (2013). Embryonic stem cell self-renewal pathways converge on the transcription factor Tfcp2l1. *EMBO J.* **32**, 2548–60.

Ying, Q.-L. and Smith, A. (2017). The Art of Capturing Pluripotency: Creating the Right Culture. *Stem cell reports* **8**, 1457–1464.

Ying, Q. L., Wray, J., Nichols, J., Batlle-Morera, L., Doble, B., Woodgett, J., Cohen, P. and Smith, A. (2008). The ground state of embryonic stem cell self-renewal. *Nature* **453**, 519–523.

Figures

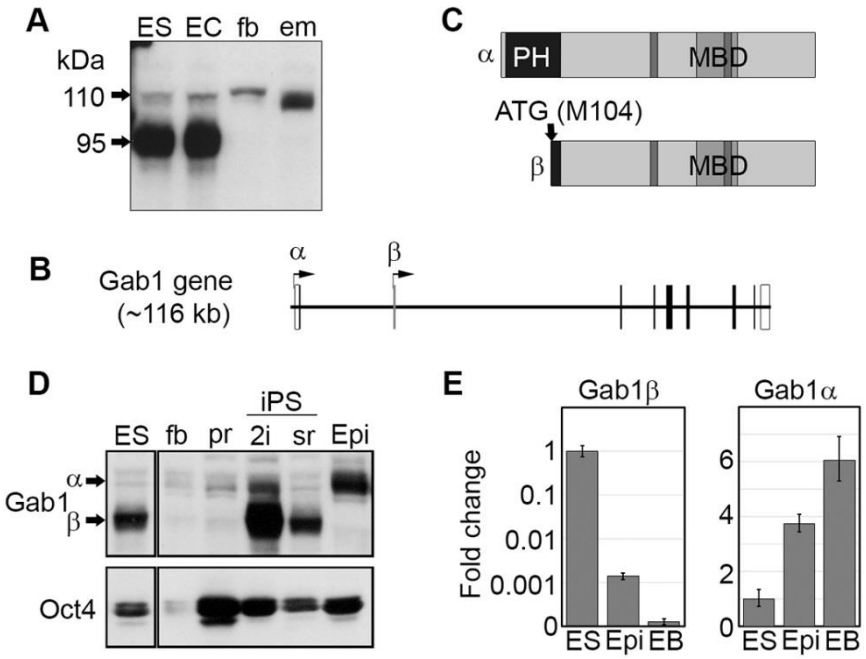

FIGURE 1. **Expression profile of a novel Gab1 variant protein**. (A) Gab1 Western blot analysis of whole cell lysates from ESC (ES), embryonal carcinoma (EC), 10T1/2 embryonic fibroblasts (fb) and pooled E12.5 embryo tissues (em). The positions of the 110 and 95 kDA Gab1 proteins are identified. (B) Schematic of the Gab1 gene locus, showing the location of the transcription start sites for Gab1α and Gab1β, and the exons. (C) Schematic showing the structure of Gab1α and Gab1β proteins. Dark grey, and light grey designated areas are proline rich regions and the Met binding domain (MBD), respectively. (D) Gab1 and Oct4 Western blots of whole cell lysates of ESC (ES), primary embryonic fibroblasts (fb), pre-iPS cells (pr), iPSCs reprogrammed in 2i medium (2i) or serum/LIF medium (sr) and an epiblast stem cell line (Epi). (E) Quantitative RT-PCR analysis of Gab1β and Gab1α expression in ESCs (ES) transitioned into epiblasts stem cells (Epi) and embryoid bodies (EB). Results represent means +/- 1 SD from one experiment. Expression is normalised relative to the level in ESCs.

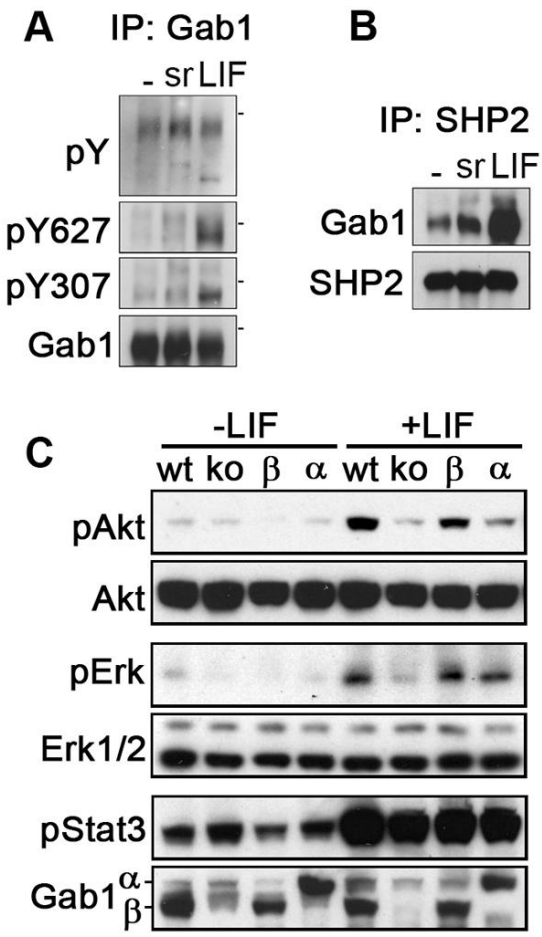

FIGURE 2. **Gab1β as an ESC signal transducer.** (A) Western blot of Gab1 immunoprecipitates from unstimulated ESC (-) or ESCs stimulated with serum (sr) or LIF (lf) for 10 minutes, probed with Gab1pY627, Gab1pY307, phosphotyrosine, and Gab1 specific antibodies. The dashes identify 100kDa. (B) Western blot of SHP2 immunoprecipitates from cells treated as in (A) probed with Gab1 and SHP2 antibodies. (C) Western blot of cell lysates from wild type ESC, and Gab1β knock-out ESC line stably transfected with empty vector (-/-), Gab1β, and Gab1α expression vectors, unstimulated or following stimulation with LIF for 15 minutes. The blot was incubated with antibodies to phospho-Akt, Akt, phospho-Erk, Erk1/2, phospho-Stat3 and Gab1.

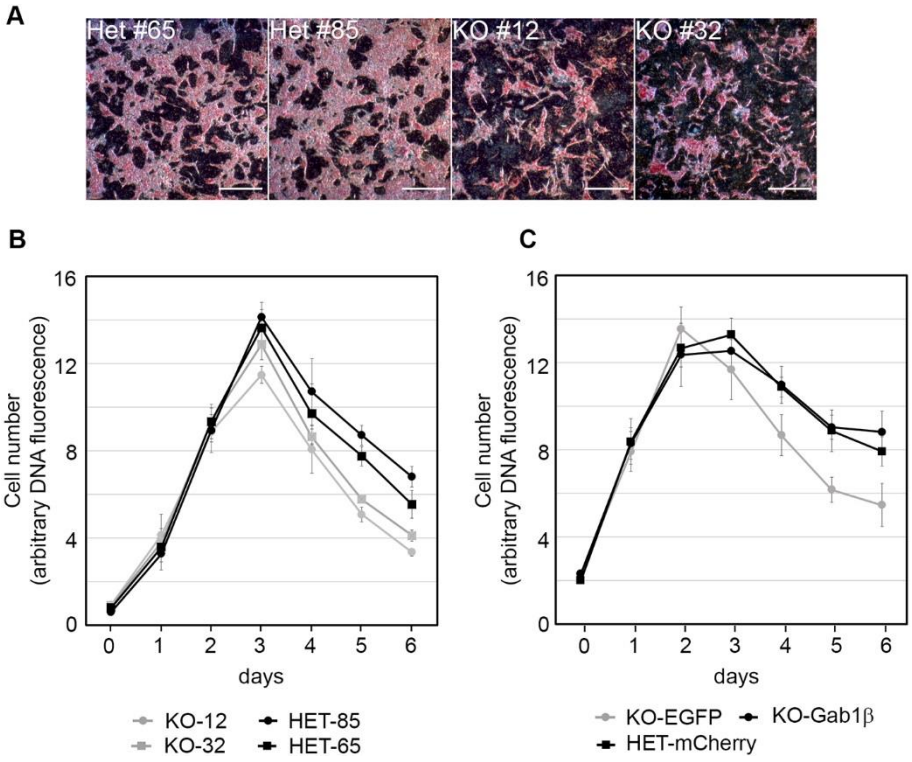

FIGURE 3. **Gab1β function in ESC.** (A) Undifferentiated ESC identified by alkaline phosphatase activity (pink stain) in two Gab1β heterozygous (HET) and two Gab1β knock-out (KO) E14Tg2a cell lines 5 days after plating. Scale bars = 200 μm (B) Growth curves of Gab1β heterozygous (HET) and Gab1β knock-out (KO) E14Tg2a cell lines measured by DNA-dependent fluorescence in live cells. Cells were plated at a density close to that for routine passaging of ESCs (6 x10^4 cells/cm^2) and the DNA fluorescence was measured daily for 6 days. The data represents the mean of three independent experiments +/- s.e.m. Statistical analysis by t-test showed significant differences between the averages for the HET and KO lines from day 3 to day 6 ($p \leq 0.005$). (C) Growth curves performed as described in (B) with pooled transfected ESCs that were Gab1β heterozygous (HET-mCherry), Gab1β knock-out (KO-EGFP) and Gab1β knock-outs stably expressing Gab1β from a cDNA expression vector (KO-Gab1β). t-test analysis showed significant differences between the KO-EGFP and KO-Gab1β lines from day 4 to day 6 ($p<0.0001$), but not between HET-mCherry and KO-Gab1β cells.

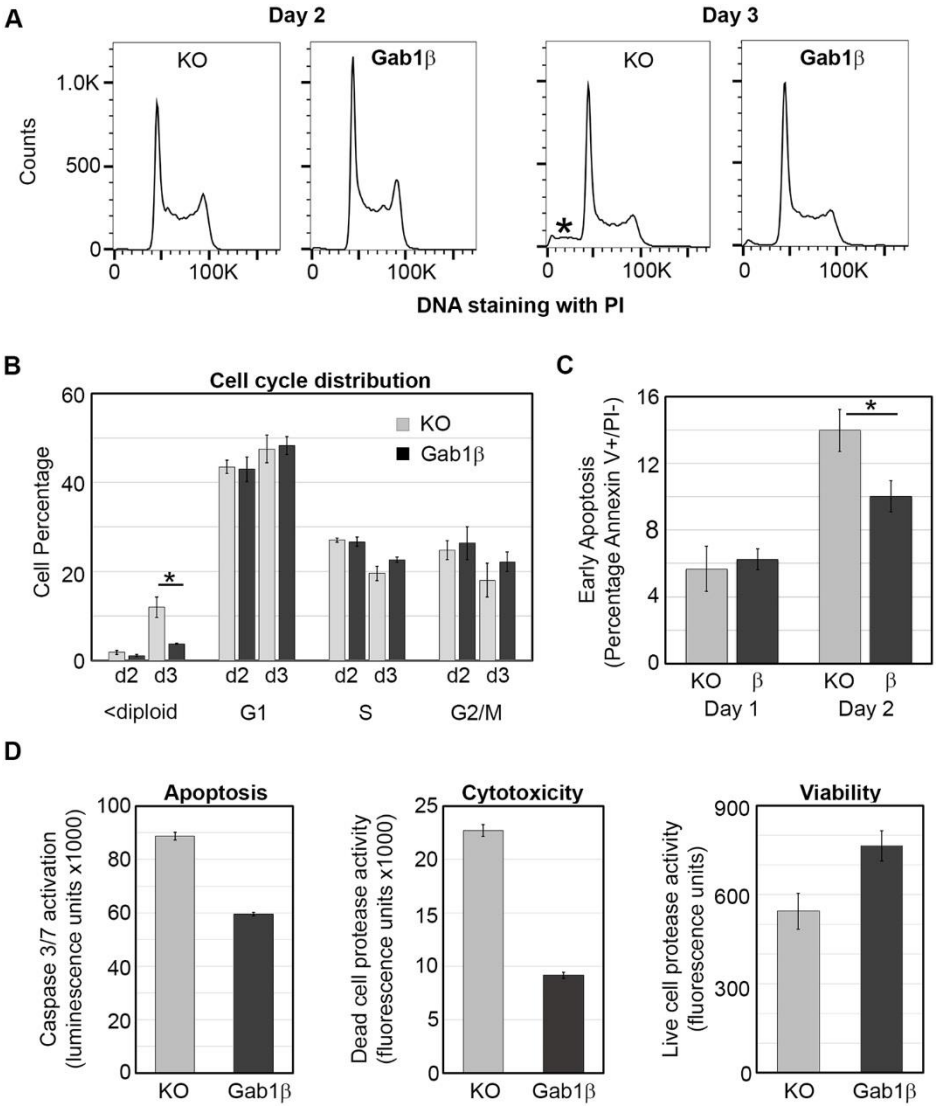

FIGURE 4. **Gab1β regulation of ESC cell cycle and apoptosis.**

(A) Cell cycle analysis of Gab1β expressing or non-expressing ESC by flow cytometry. Triplicate ESC samples were collected at day 2 and 3 of culture, fixed and stained using propidium iodide, and analysed by flow cytometry. Representative scans are shown and sub-diploid cell material is identified by the asterisk. (B) Quantitation of cell cycle distribution. Mean values of cell cycle phases +/- 1 SD generated from three independent cultures (* t-test $p<0.005$). (C) Flow cytometry of Annexin V staining in day 1 and day 2 ESC cultures. Grey and black bars are values from Gab1β KO and Gab1β expressing (Gab1β KO + Gab1β cDNA vector) ESCs respectively (* t-test $p<0.005$). (D) Apoptosis, cytotoxicity and viability assays of day 2 cultures of Gab1β KO and Gab1β

expressing ESCs. Values are means of 4 biological replicates +/- 1 SD (apoptosis and cytotoxicity t-tests $p<0.0001$; viability t-test $p<0.005$).

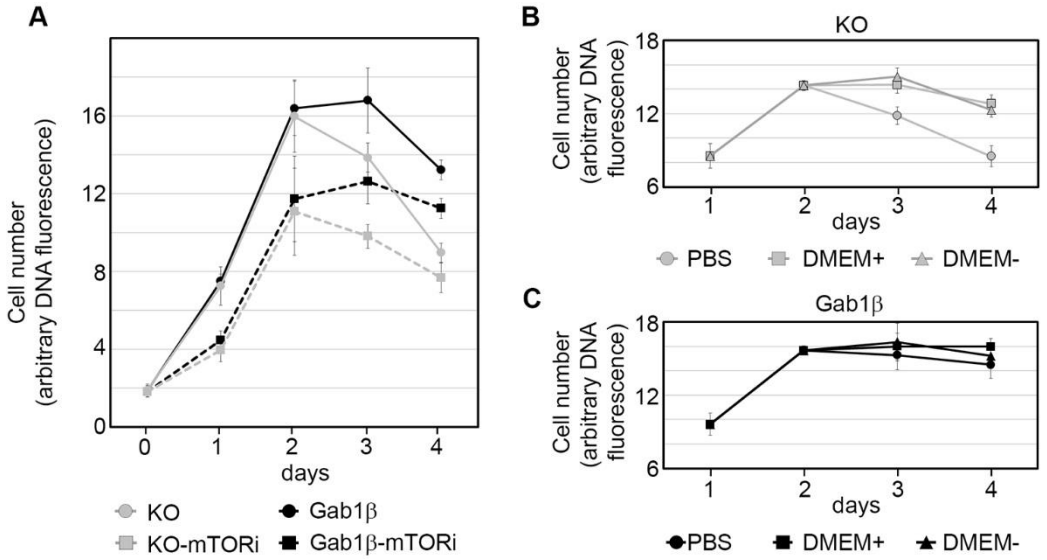

FIGURE 5. **Gab1β and ESC response to nutrient availability.**

(A) Growth profiles of Gab1β KO and Gab1β expressing ESCs treated with 25 nM mTOR inhibitor INK128 (mTORi). Values are means of three independent experiments +/- s.e.m. (B, C) Growth of Gab1β KO and Gab1b expressing ESC cultures supplemented on day 2 with either 10 μl PBS, regular DMEM (+), or DMEM (-) lacking glucose, glutamine, and sodium pyruvate. Values are means of three biological replicates +/- 1 SD.

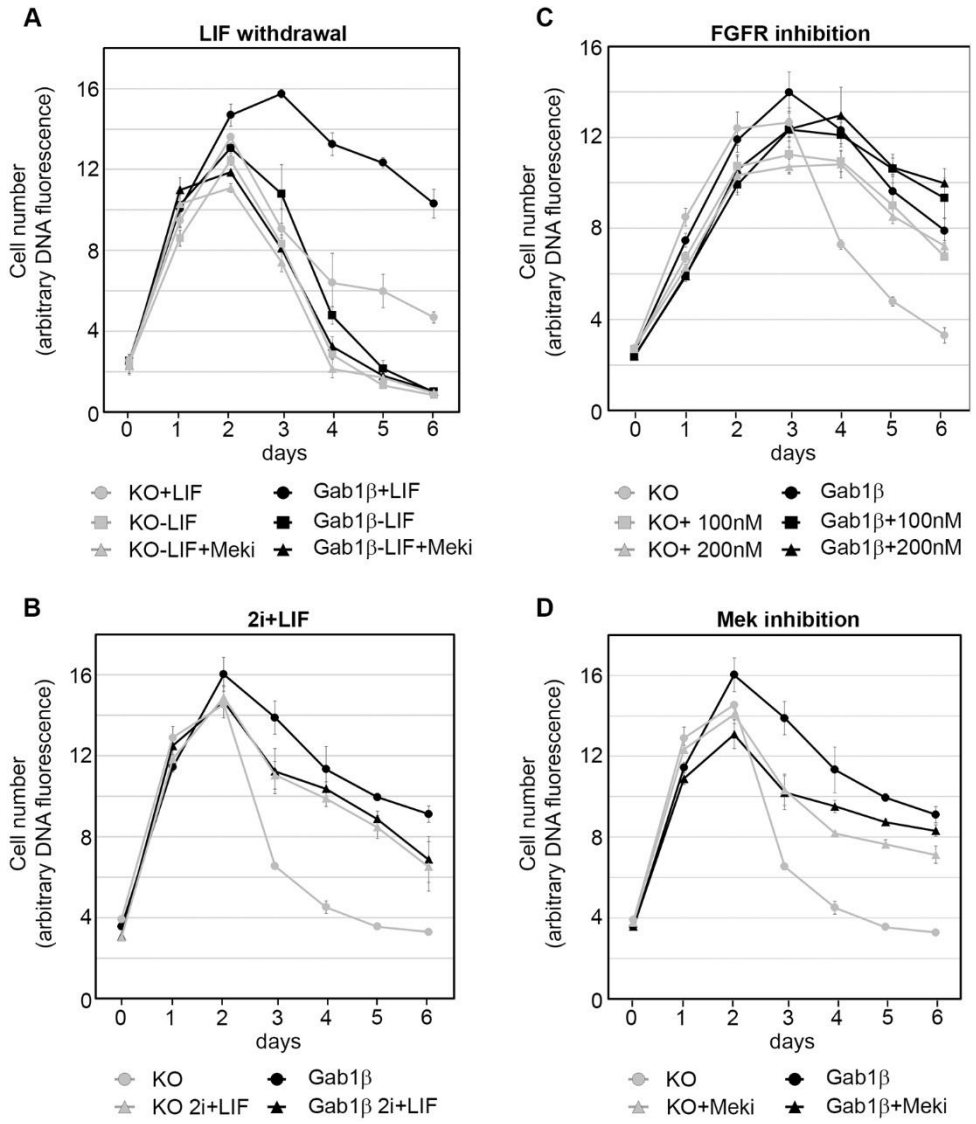

FIGURE 6. **Gab1β mediated ESC survival dependency on LIF, and rescue by Mek inhibition.** Growth profiles of Gab1β KO and Gab1β expressing ESCs cultured in: (A) the presence or absence of LIF (+/- 1 μM PD0325901 Mek inhibitor); (B) 2i (1 μM PD0325901 Mek inhibitor, 3 μM CHIR99021 GSK3 inhibitor) +LIF serum free medium; (C) +/- FGFR inhibitor PD173074 (one experiment with quadruplicate biological samples; and (D) +/- 1 μM PD0325901 Mek inhibitor. Data points in graphs A, B and D represent the means of three independent experiments +/- s.e.m. Data points in graph C represent the means from four biological replicates in one experiment. For all graphs t-tests showed

statistically significant differences between serum+LIF treated KO and KO+Gab1β control lines at days 4-6 ($p \leq 0.0001$), and between KO control and KO treated cells ($p \leq 0.0001$).

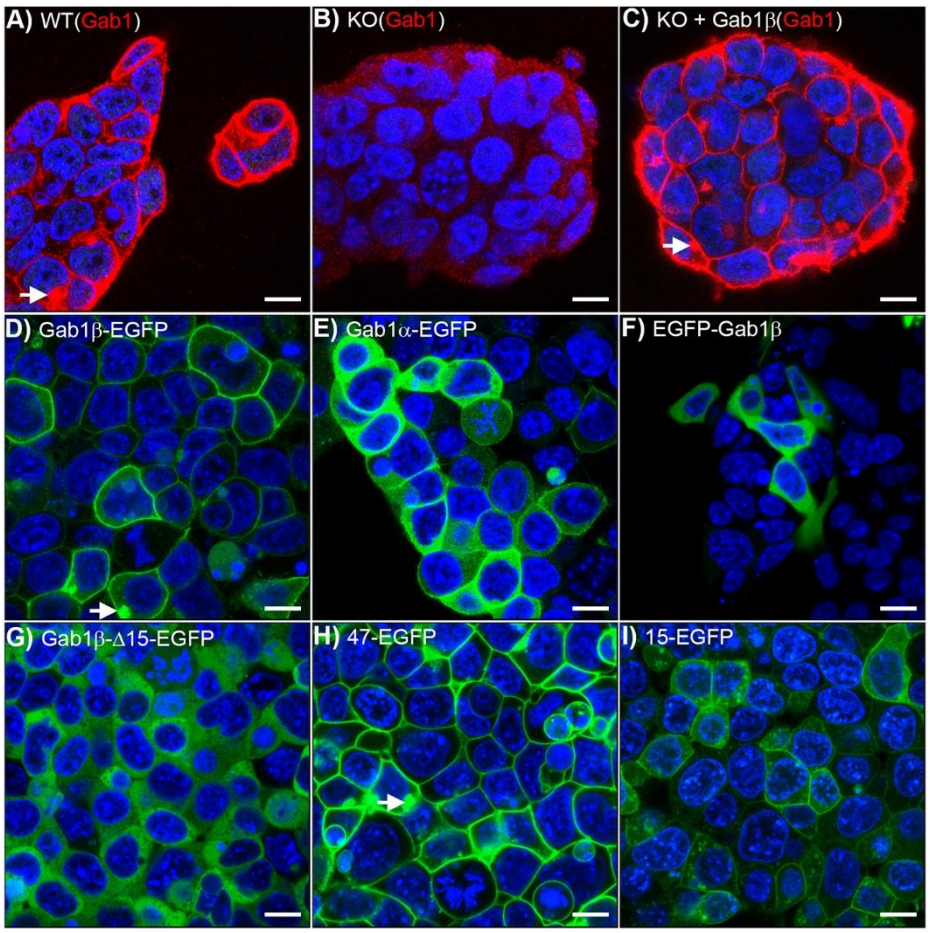

FIGURE 7. **Localisation of Gab1β at the cell membrane**. Confocal images of (A) Wild type ESC, (B) Gab1β knock-out ESC and (C) Gab1β knock-out ESC stably transfected with a Gab1β cDNA expression vector, immunostained with antibodies against Gab1 (red) and counter-stained for DNA with Dapi (Blue). Confocal images of EGFP fluorescence in ESC stably expressing the following Gab1-EGFP fusion proteins: (D) Gab1β-EGFP; (E) Gab1α-EGFP; (F) N-terminal EGFP-Gab1β; (G) Gab1β-EGFP fusion lacking 15 N-terminal amino acids; (H) the 47 N-terminal amino acid peptide of Gab1β fused to EGFP; and (I) 15 N-terminal amino-acid peptide of Gab1β fused to EGFP. White arrows highlight consitently observed intracellular accumulations of Gab1β proteins. Scale bars = 10 μm.

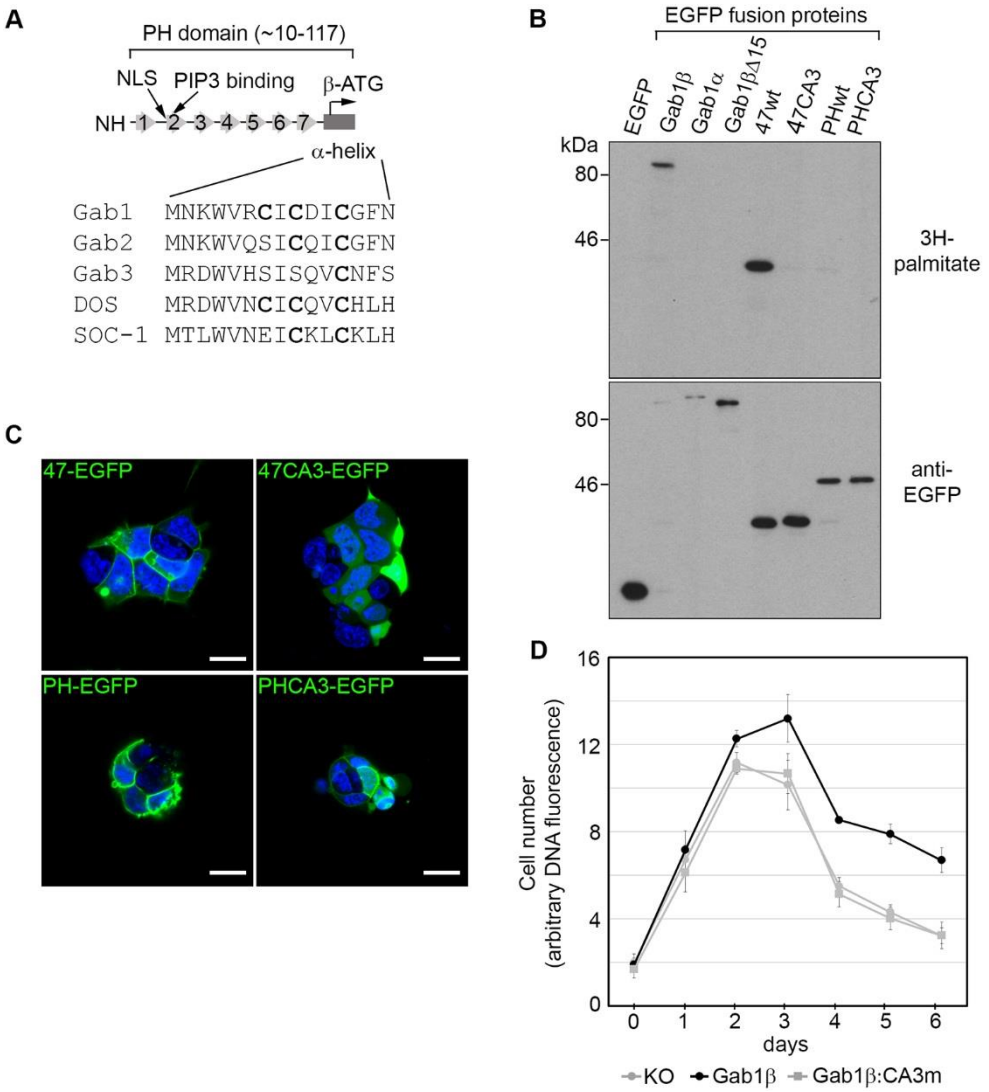

FIGURE 8. **N-terminus of Gab1β directs palmitoylation and is required for membrane localisation and function.** (A) Schematic outlining the structure of the Gab1 PH domain and comparison of the N-terminus of Gab1β with corresponding regions of other Gab-related proteins. The arrangement of the seven β-sheets and the α-helix, and relative positions of a putative nuclear localisation sequence and PIP3 binding residues are shown. Cysteines within the α-helix are highlighted in bold. (B) EGFP immunoprecipitates from ESC stably transfected with EGFP or Gab1-EGFP fusion proteins cultured overnight with 3H- palmitate, were fractionated on an SDS protein gel, transferred to a filter and autoradiographed (upper panel) and probed for EGFP protein (lower

panel). CA3 designation identifies variants in which the three N-terminal cysteines of Gab1β are substituted with alanine (C) Confocal images of EGFP fluorescence in ESC transfected with the 47-EGFP, 47CA3-EGFP, PH domain-EGPF and PH domain CA3-EGPF fusion proteins (counter-stained with Dapi). Scale bars = 10 μm. (D) Growth curves of Gab1β knock-out (KO) ESC and Gab1β knock-out ESCs stably transfected with either Gab1β wild-type or CA3 mutant cDNA expression vectors. The graphs represent the means obtained from three independent experiments +/- s.e.m. t-test analysis showed significant differences between the KO and KO-Gab1β lines from day 4 to day 6 ($p<0.0001$), but not between KO and KO-Gab1β:CA3m cells

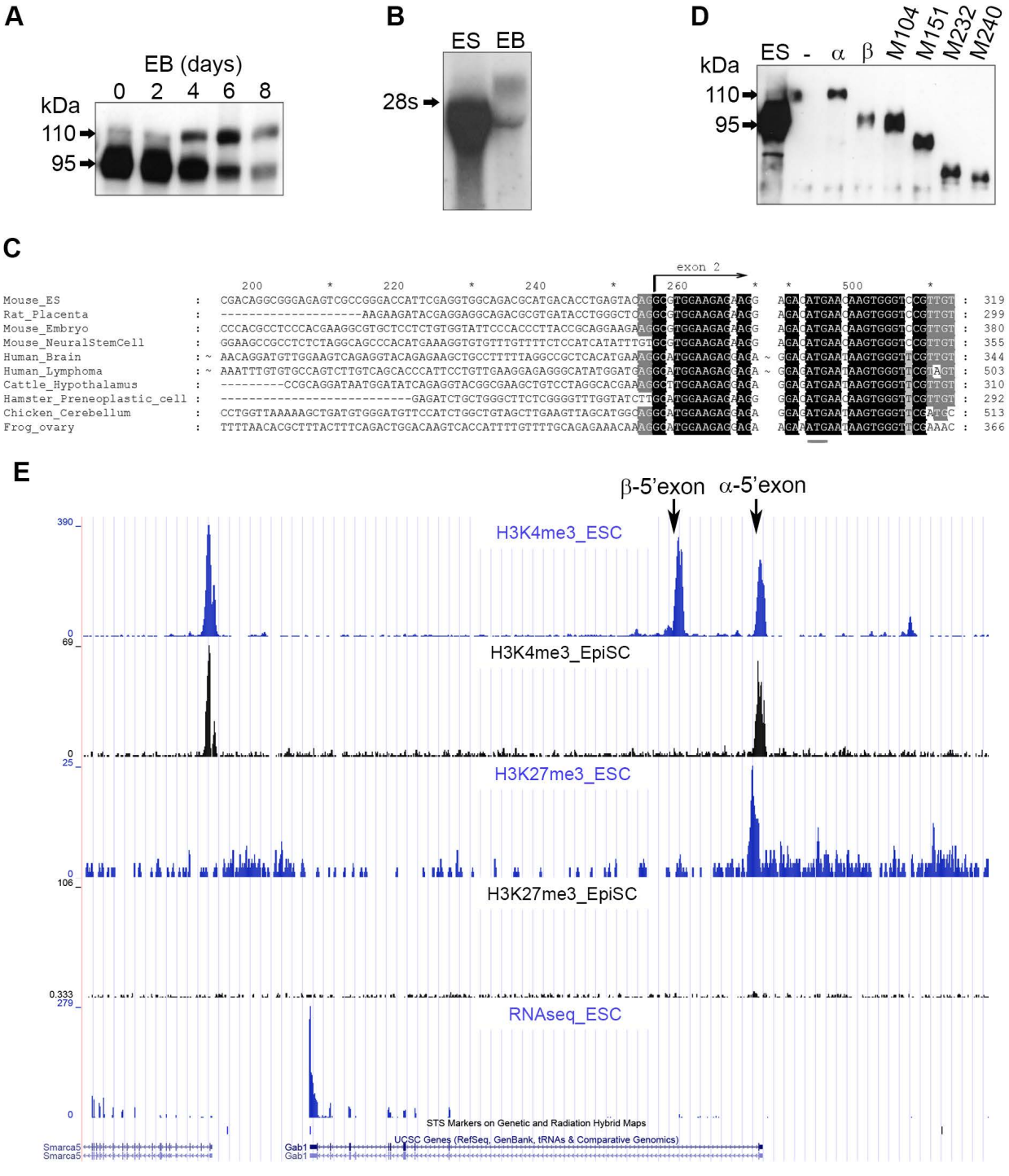

SUPPLEMENTARY FIGURE 1. **Expression of a novel form of Gab1.** (A) Western blot showing Gab1 protein expression in whole cell lysates prepared from undifferentiated ESCs, ESCs at 2, 4, 6 and 8 days during embryoid body differentiation in suspension culture. (B) Northern blot of total RNA prepared from ESC and day 8 embryoid body hybridised with Gab1 cDNA probe. The position of the 28S ribosomal RNA (approx. 5 kb) identified by ethidium bromide staining of the filter prior to hybridisation is indicated (C) Alignment of Gab1 ESTs which have a non-coding 5' exon analogous to Gab1β that have been identified in different species. (D) Gab1 proteins produced by COS7 cells transfected with Gab1α and β cDNAs where translation initiates at methionines 104, 151, 232 or 240. (E) H3K4me3 and H3K27me3 histone modifications at the mouse *Gab1* locus in ESC and EpiSCs visualised in the UCSC genome browser. Whereas a region adjacent to the Gab1β exon is enriched for the H3K4me3 mark indicative of active transcription, the corresponding region at the Gab1α exon is enriched for both active and repressed (H3K27me3) modifications (bivalent). The RNA-seq track in ESC demonstrates that the Gab1 locus is transcriptionally active (from right to left).

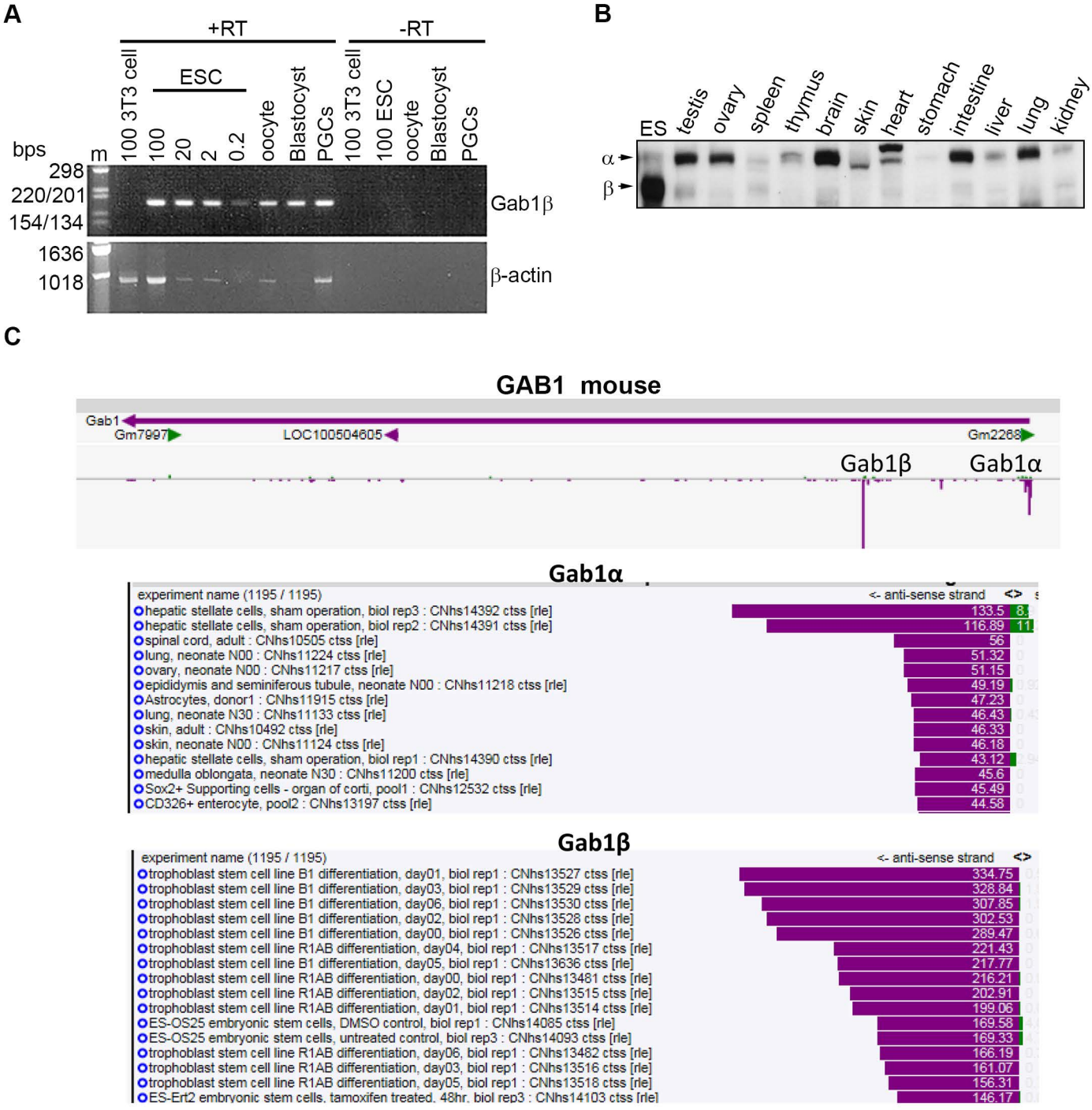
A
+RT
-RT
100 3T3 cell
ESC
100
20
2
0.2
oocyte
Blastocyst
PGCs
100 3T3 cell
100 ESC
oocyte
Blastocyst
PGCs
bps
m
298
220/201
154/134
Gab1β
1636
1018
β-actin
B
ES
testis
ovary
spleen
thymus
brain
skin
heart
stomach
intestine
liver
lung
kidney
α
β
C
GAB1 mouse
Gab1
Gm7997
LOC100504605
Gm2268
Gab1β
Gab1α
Gab1α
experiment name (1195 / 1195)
<- anti-sense strand
hepatic stellate cells, sham operation, biol rep3 : CNhs14392 ctss [rle] 133.5
hepatic stellate cells, sham operation, biol rep2 : CNhs14391 ctss [rle] 116.89
spinal cord, adult : CNhs10505 ctss [rle] 56
lung, neonate N00 : CNhs11224 ctss [rle] 51.32
ovary, neonate N00 : CNhs11217 ctss [rle] 51.15
epididymis and seminiferous tubule, neonate N00 : CNhs11218 ctss [rle] 49.19
Astrocytes, donor1 : CNhs11915 ctss [rle] 47.23
lung, neonate N30 : CNhs11133 ctss [rle] 46.43
skin, adult : CNhs10492 ctss [rle] 46.33
skin, neonate N00 : CNhs11124 ctss [rle] 46.18
hepatic stellate cells, sham operation, biol rep1 : CNhs14390 ctss [rle] 43.12
medulla oblongata, neonate N30 : CNhs11200 ctss [rle] 45.6
Sox2+ Supporting cells - organ of corti, pool1 : CNhs12532 ctss [rle] 45.49
CD326+ enterocyte, pool2 : CNhs13197 ctss [rle] 44.58
Gab1β
experiment name (1195 / 1195)
<- anti-sense strand
trophoblast stem cell line B1 differentiation, day01, biol rep1 : CNhs13527 ctss [rle] 334.75
trophoblast stem cell line B1 differentiation, day03, biol rep1 : CNhs13529 ctss [rle] 328.84
trophoblast stem cell line B1 differentiation, day06, biol rep1 : CNhs13530 ctss [rle] 307.85
trophoblast stem cell line B1 differentiation, day02, biol rep1 : CNhs13528 ctss [rle] 302.53
trophoblast stem cell line B1 differentiation, day00, biol rep1 : CNhs13526 ctss [rle] 289.47
trophoblast stem cell line R1AB differentiation, day04, biol rep1 : CNhs13517 ctss [rle] 221.43
trophoblast stem cell line B1 differentiation, day05, biol rep1 : CNhs13636 ctss [rle] 217.77
trophoblast stem cell line R1AB differentiation, day00, biol rep1 : CNhs13481 ctss [rle] 216.21
trophoblast stem cell line R1AB differentiation, day02, biol rep1 : CNhs13515 ctss [rle] 202.91
trophoblast stem cell line R1AB differentiation, day01, biol rep1 : CNhs13514 ctss [rle] 199.06
ES-OS25 embryonic stem cells, DMSO control, biol rep1 : CNhs14085 ctss [rle] 169.58
ES-OS25 embryonic stem cells, untreated control, biol rep3 : CNhs14093 ctss [rle] 169.33
trophoblast stem cell line R1AB differentiation, day06, biol rep1 : CNhs13482 ctss [rle] 166.19
trophoblast stem cell line R1AB differentiation, day03, biol rep1 : CNhs13516 ctss [rle] 161.07
trophoblast stem cell line R1AB differentiation, day05, biol rep1 : CNhs13518 ctss [rle] 156.31
ES-Ert2 embryonic stem cells, tamoxifen treated, 48hr, biol rep3 : CNhs14103 ctss [rle] 146.17

SUPPLEMENTARY FIGURE 2. **Gab1β expression profiles.** (A) Reverse transcriptase PCR analysis of Gab1β expression in embryonic cells. Gab1β expression was analysed in cDNA prepared from ESC (0.2-100 ESC equivalents), unfertilised oocytes, blastocysts and primordial germ cells (PGCs) and NIH3T3 fibroblasts (equivalent to 100 cells). Gab1β, and β-actin specific primers generated 184 bp and 939 bp amplicons, respectively. (B) Western blot of Gab1 protein expression in whole tissue lysates prepared from adult mouse. (C) Quantitative transcription start site expression at the mouse *Gab1* gene locus derived from FANTOM5 mouse Cap Analysis of Gene Expression (CAGE) data analysis. The upper sections describes the summary of transcription initiation at Gab1α and Gab1β transcription start sites (TSS) combining cumulative CAGE data from over 1000 individual mouse cell and tissue samples visualised in the ZENBU genome browser. The tissues/cell types with the highest expression (in descending order) for Gab1α and Gab1β TSS is presented as normalised tags per million counts (purple bars on right) for each sample.

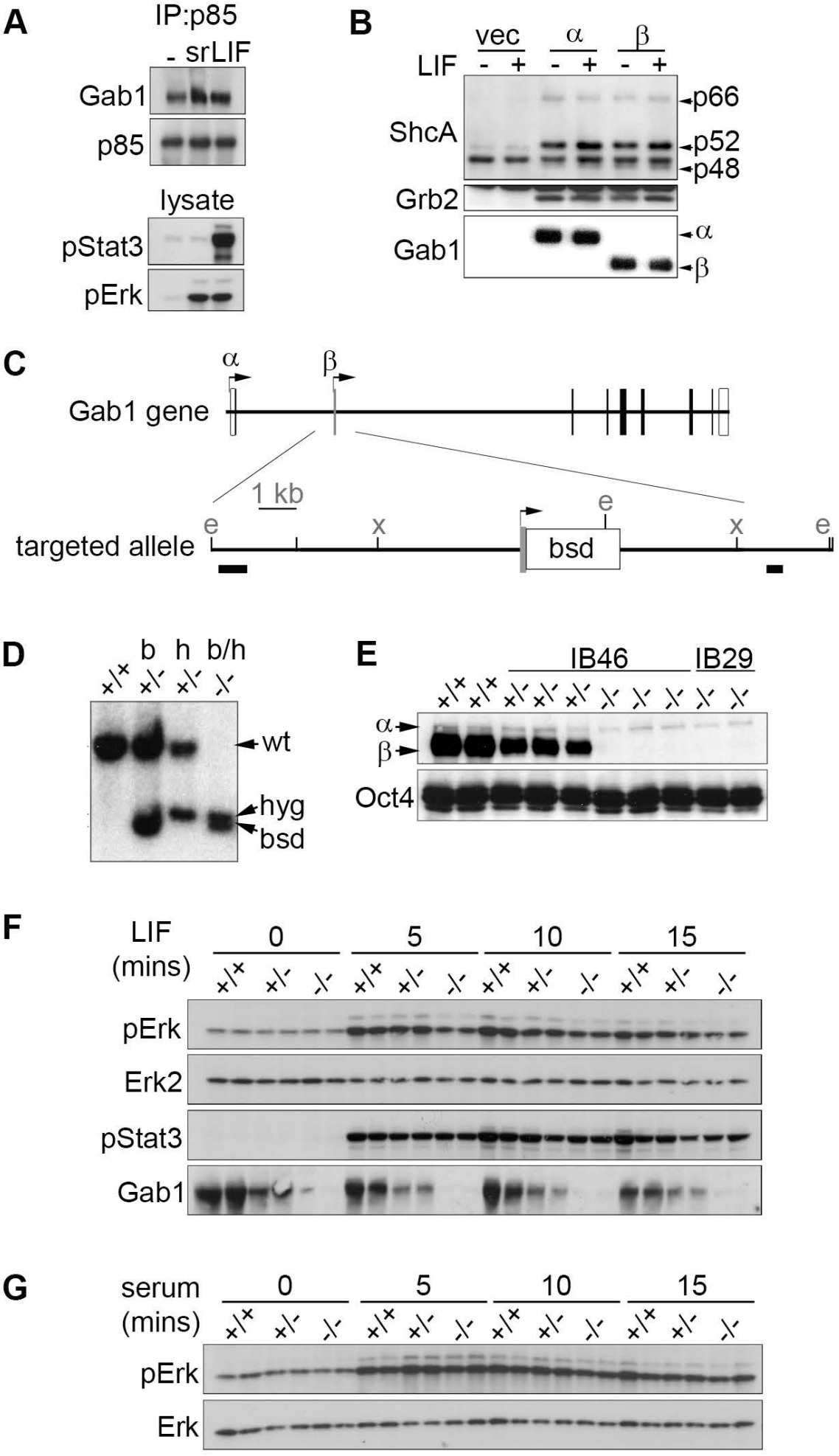

SUPPLEMENTARY FIGURE 3. **Analysis of Gab1β signalling** (A) Western blots of PI3K p85 immunoprecipitates from unstimulated ESC (-) or ESCs stimulated with serum (sr) or LIF (lf) for 10 minutes, incubated with Gab1 and p85 antibodies; and cell lysates generated in (A) incubated with antibodies against phospho-Stat3 (Y705) and phospho-Erk. (B) Western blot of anti-myc immunoprecipitates prepared from ESCs transfected with empty (vec), myc epitope-tagged Gab1α and myc epitope-tagged Gab1β expression vectors, incubated with antibodies against Shc, Grb2 and Gab1. (C) Schematic showing the Gab1 gene locus and targeting vector used to insert the blastocydin^{R} selection cassette into the Gab1β first exon. Location of external probes used to screen for targeted insertion of the selection cassette are shown as black bars. (D) Southern blot of EcoRV digested genomic DNA prepared from IOUD2 Gab1β wild-type ESC (+/+), heterozygous Gab1β-blastocidin^{R}, Gab1β-hygromycin^{R} clones (+/-) and a double targeted Gab1β-blastocidin^{R}/Gab1β-hygromycin^{R} homozygous Gab1β null clone (-/-), hybridised with a ^{32}P-labelled Gab1 5' external probe. (E) Western blot of Gab1 and Oct4 protein expression in whole cell lysates from Gab1β wildtype, Gab1β heterozygous and Gab1β null ESCs. (F, G) Western blot analysis of phospho-Erk, Erk2 and phospho-Stat3 (Y705) in cell lysates prepared from Gab1β wild-type, heterozygous and homozygous null ESCs following stimulation with LIF or Serum for 0,5,10 and 15 minutes.

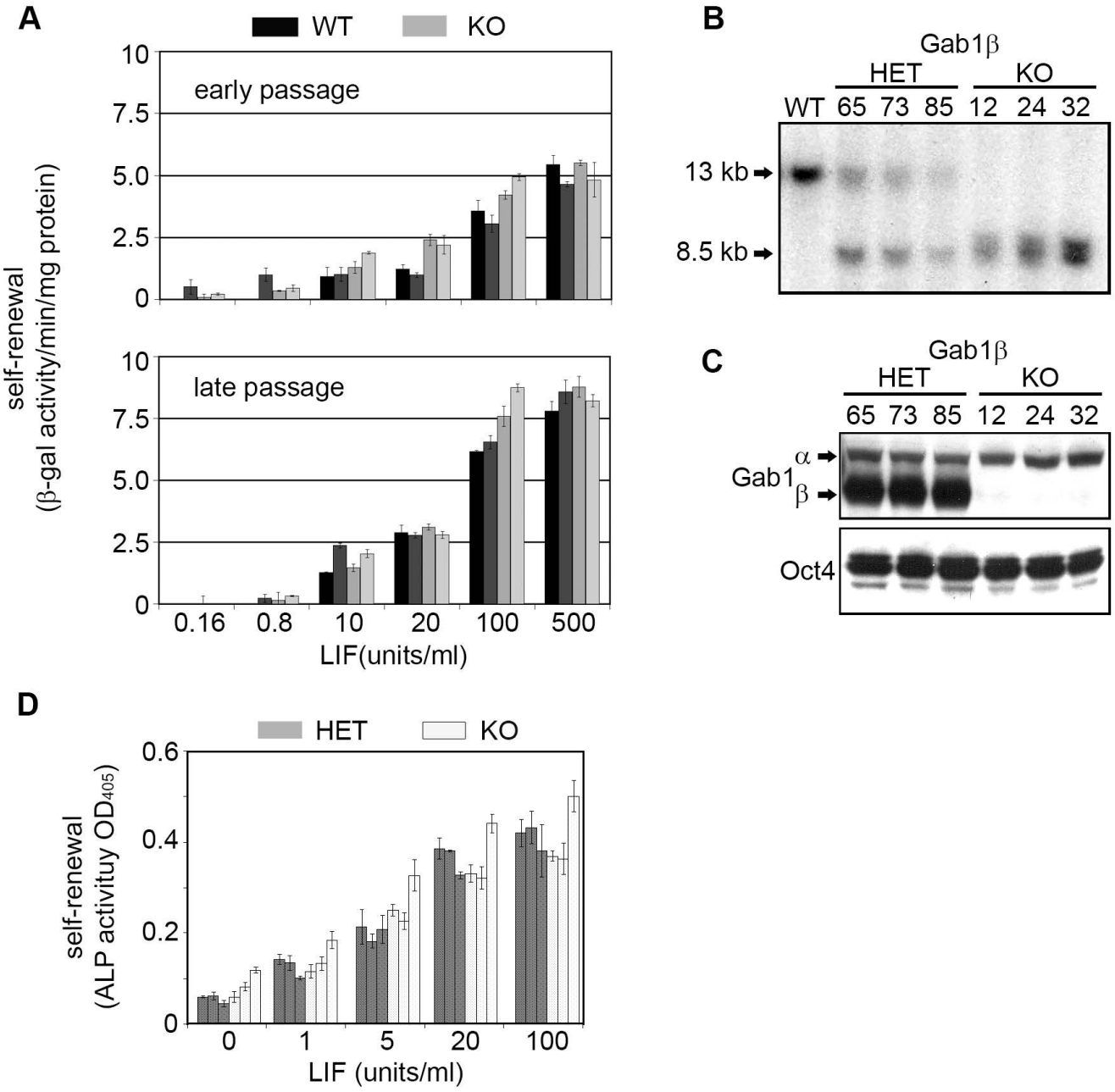

SUPPLEMENTARY FIGURE 4. **Role of Gab1β in ESC self-renewal.** (A) Self-renewal response to LIF titration in two Gab1β wild-type (darker shaded bars) and Gab1β KO (light shaded grey bars) IOUD2 cell lines as measured by *pou5F1*-LacZ activity in day 5 low density cultures at early and late passages. Data represents the means ± SD of three biological replicates. (B) Southern blot of EcoRV digested genomic DNA prepared from E14Tg2a wild-type ESC (WT), three heterozygous Gab1β-hygromycin^R clones (HET) and three Gab1β-blastocidin^R/Gab1β-hygromycin^R homozygous Gab1β null clones (KO) , hybridised with a ^{32}P-labelled Gab1 5' external probe. (C) Western blot of Gab1 and Oct4 protein expression in cell lysates prepared from E14Tg2a Gab1β HET and KO clones. (D) Self-renewal response to LIF titration in Gab1β HET (dark bars) and Gab1β KO (white bars) E14Tg2a ESCs as measured by alkaline phosphatase activity. Data represents the means ± SD of three biological replicates.

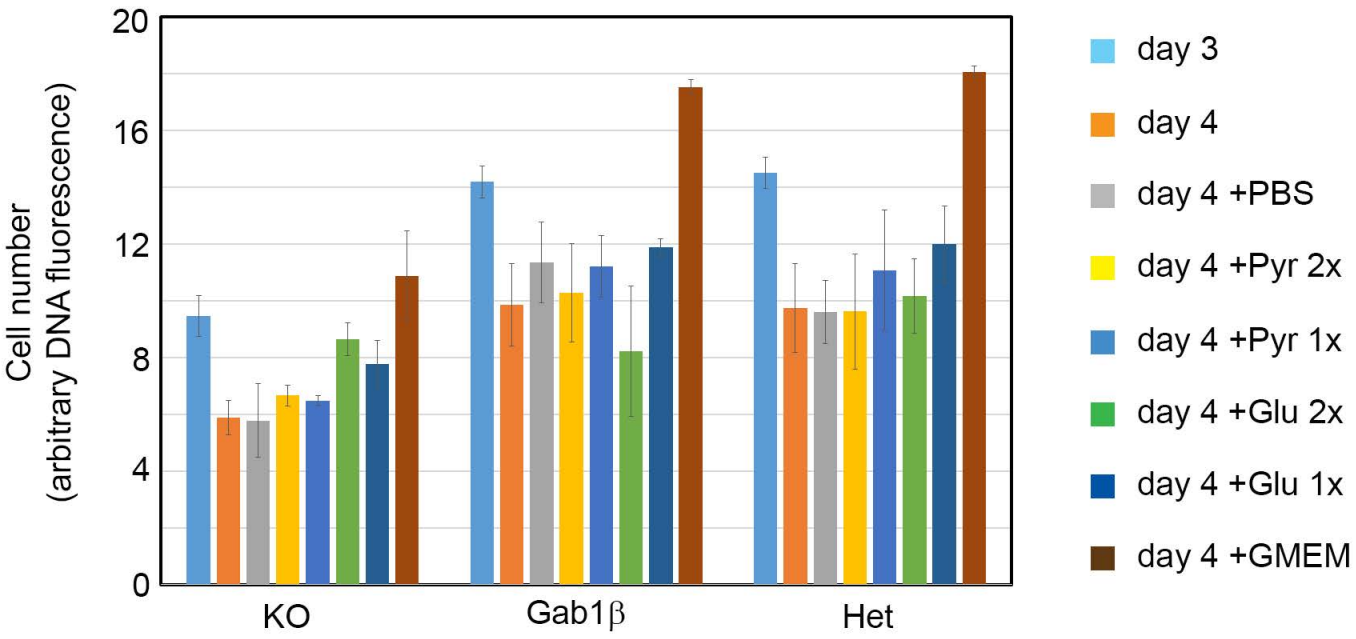

SUPPLEMENTARY FIGURE 5. **Assessment of the factors that may limit ESC growth in near-confluent cultures.** (A) Growth of Gab1β KO, Gab1β expressing, and Gab1β Heterozygous ESCs at 3 days in culture, and then after supplementation with 10 μl PBS or PBS containing 1 mM or 2 mM Sodium Pyruvate, or 2 mM or 4 mM Glutamine, or 10 μl GMEM and cultured for a further 24 hrs.

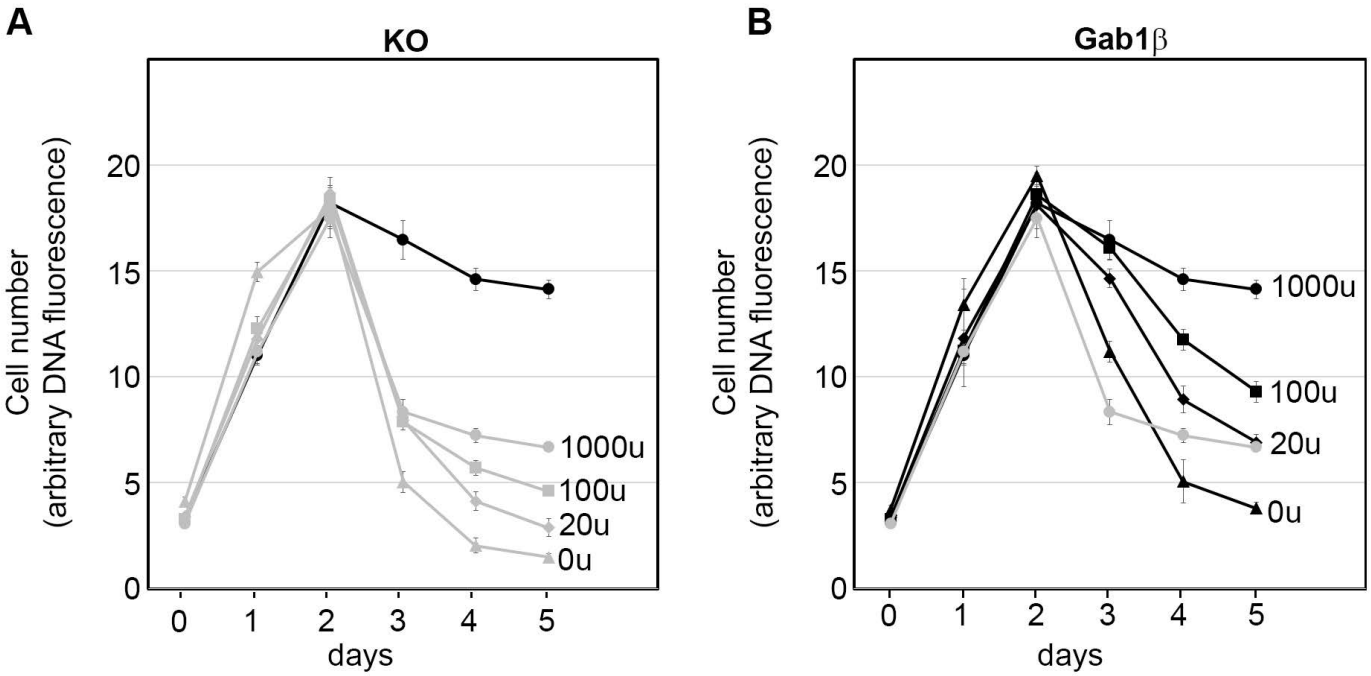

SUPPLEMENTARY FIGURE 6. **Effect of LIF titration on growth of Gab1β KO and Gab1β expressing ESCs.** Growth profiles of (A) Gab1β KO and (B) Gab1β expressing ESCs cultured in the presence 0, 20, 100 and 1000 units/ml of LIF for 6 days. The values represent the means of four biological replicate cultures +/- SD. For reference, the dark line in (A) is comprised of the values obtained from the Gab1β expressing ESCs grown in 1000 units/ml LIF , and in (B) the grey line is the KO cells grown in 1000 units/ml LIF.